Journal of
Medicinal Chemistry

Article

The discovery of an orally bioavailable pan-#v integrin inhibitor for idiopathic pulmonary fibrosis.

Niall A Anderson, Sebastien Campos, Sharon Butler, Royston C. B. Copley, Ian Duncan, Stephen Harrison, Joelle Le, Rosemary Maghames, Aleix Pastor-Garcia, John M. Pritchard, James E. Rowedder, Claire E. Smith, Jack Thomas, Giovanni Vitulli, and Simon J. F. Macdonald

J. Med. Chem., **Just Accepted Manuscript** • DOI: 10.1021/acs.jmedchem.9b00962 • Publication Date (Web): 09 Sep 2019

Just Accepted

is published by the American Chemical Society. 1155 Sixteenth Street N.W., Washington, DC 20036

The discovery of an orally bioavailable pan αv integrin inhibitor for idiopathic pulmonary fibrosis.

Niall A. Anderson,* Sebastien Campos,[≠] Sharon Butler, Royston C. B. Copley, Ian Duncan, Stephen Harrison, Joelle Le, Rosemary Maghames, Aleix Pastor-Garcia, John M. Pritchard, James E. Rowedder, Claire E. Smith, Jack Thomas, Giovanni Vitulli, Simon J.F. Macdonald

*GlaxoSmithKline Medicines Research Centre, Gunnels Wood Road, Stevenage, SG1 2NY, UK

KEYWORDS Integrin, pan αv, oral bioavailability, IPF

ABSTRACT: The heterodimeric transmembrane αv integrin receptors have recently emerged as potential targets for the treatment of idiopathic pulmonary fibrosis. Herein we describe how subtle modifications of the central aromatic ring of a series of phenylbutyrate-based antagonists of the vitronectin receptors αvβ3 and αvβ5 significantly change the biological activities against αvβ6 and αvβ8. This resulted in the discovery of a pan αv antagonist (compound **39** – 4 to 40 nM for the integrin receptors named above) possessing excellent oral pharmacokinetic properties in rats (with of clearance 7.6 mL/min/kg and bioavailability 97%).

INTRODUCTION

It is estimated around 45% of deaths in the industrialised world are attributable to some sort of fibrotic disease.[1] One of these, idiopathic pulmonary fibrosis (IPF) is a chronic, progressive disease of the interstitial lung thought to be caused by repeated injury or insult.[2,3] After diagnosis, the average life expectancy varies from three to five years depending on the severity[4,5] and the mortality rate exceeds that of many cancer indications.[6,7] Current estimates suggest it is the seventh biggest killer in the UK, killing around 5,000 people every year and there has been a six–fold increase in deaths since 1979.[8] Pirfenidone and nintedanib are the only two drugs specifically approved for the treatment of IPF. Both drugs have demonstrated to significantly slow the progression of IPF,[9,10] but neither is a cure. There is therefore, a pressing need for novel efficacious treatments for IPF.

Integrins are a family of heterodimeric transmembrane receptors, each consisting of an α and β subunit.[11] The genome encodes eighteen α subunits and eight β subunits that heterodimerise to form twenty four αβ integrin combinations. Of these twenty four integrins, eight (including all five αv containing integrins: αvβ1, αvβ3, αvβ5, αvβ6 and αvβ8) bind ligands through an arginine-glycine-aspartic acid (RGD) sequence.[12] The αvβ6 receptor is overexpressed in the lung tissue of fibrotic patients and inhibition of the receptor with a monoclonal antibody has been shown to prevent pulmonary fibrosis in animal models.[13] Moreover, whilst mice that do not express the αvβ6 receptor develop mild inflammation in the lungs and skin, they are protected from bleomycin induced pulmonary fibrosis.[14] The integrin αvβ1 may also play a role based on it's inhibitory effect in the bleomycin model although the reported doses administered were large and the compound used has been shown to inhibit other integrins.[15] In contrast, there is evidence that the integrins αvβ3 and αvβ5 are not involved in lung fibrosis[16] although they may play a role in asthma and COPD.[17] Obtaining exquisite selectivity for any particular integrin can be difficult due to similarities in some of the binding sites so importantly, pan αv inhibitors (compounds that inhibit the αv integrins namely αvβ3, αvβ5, αvβ6 and αvβ8 within 1 log unit) such as **CWHM12** (Figure 1) have also been shown to be protective in the bleomycin fibrosis model.[18] Consequently, the αv integrins and αvβ6 in particular have been identified as a key player in the development of IPF and inhibitors could represent efficacious new treatments for this disease. This has led to renewed interest in integrin inhibitors[12,19, 20, 21] and a selective inhaled αvβ6 small molecule GSK3008348 clinical candidate has recently been described.[22] However only a few small molecule pan αv compounds have been disclosed (such as **CWHM12**) which typically feature high numbers of H-bond donors/acceptors or have molecular weight in excess of 500 Daltons.[12] Described here is the discovery of a pan αv compound with good oral bioavailability and more commensurate drug-like properties.

RESULTS AND DISCUSSION

With the aim of developing drugs for the treatment of restenosis following percutaneous transluminal coronary angioplasty, a research group at GlaxoSmithKline previously reported the discovery of phenyl-butyrate-based antagonists of the vitronectin receptors αvβ3 and αvβ5 with excellent rat pharmacokinetics following oral administration (**1**, Figure 1).[23]

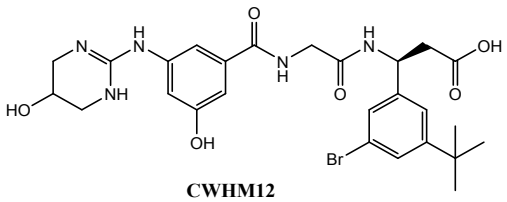

CWHM12

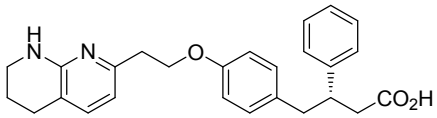

1

Figure 1. Structure of **CWHM12** and **1**

Further profiling of the racemate of **1** (analog **2**) in fluorescence polarisation (FP) αvβ3, αvβ5, αvβ6 and αvβ8 binding assays (see Supporting Information) confirmed the good activity of this template for the vitronectin receptors αvβ3 and αvβ5 (Table 1). Moreover, it demonstrated that this compound possessed significant selectivity (>600 fold) over the integrin receptors αvβ6 and αvβ8. Cross-screening of a selection of compounds prepared as part this phenyl-butyrate-based antagonist programme revealed that introduction of an aniline nitrogen in the central aromatic ring and a fluorine in the *meta* position of the right hand side aryl ring (**3**, Table 1) increased the αvβ6 binding affinity approximately 10-fold whilst retaining the αvβ3 and αvβ5 activities. Improvement of the αvβ6 binding affinity by substituting a similar aryl ring of a pan αv antagonist template with a *meta* fluorine has already been reported.[24] However, as the increase of activity in the literature example is only 2.5-fold and it was accompanied by an increase of activity for αvβ3 and αvβ5, we postulated that the aniline nitrogen of the central aryl ring may also contribute to the interesting structure activity relationship (SAR) differences between **2** and **3**. Finally, the increased inhibition of **3** against αvβ6 was confirmed in a cell adhesion assay[22] with potency in the region of 1 μM in contrast to the activity of **2** which is

below the assay threshold. In this communication, we report detailed SAR around the central aromatic ring of **3**, describing how subtle changes significantly affect the αvβ3, αvβ5, αvβ6 and αvβ8 activity and selectivity profiles. Combination of a suitable central ring and the correct aryl substitution on the right-hand side aryl ring resulted in the discovery of a pan αv antagonist with low clearance and excellent bioavailability in rat pharmacokinetic studies which is now described.

Table 1: Initial SAR comparing the phenylbutyrate and the phenylaminopropanoate templates (all compounds racemic)

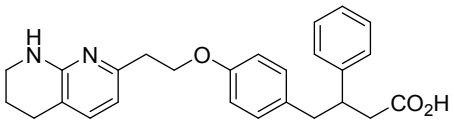

2

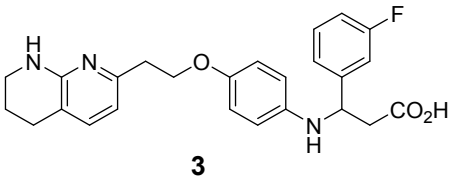

3

Cmpd	pIC$_{50}$[a]				
	$\alpha_v\beta_6$ FP	$\alpha_v\beta_3$ FP	$\alpha_v\beta_5$ FP	$\alpha_v\beta_8$ FP	$\alpha_v\beta_6$ cell adhesion
2	5.9 ± 0.09 (6)	8.7 ± 0.08 (6)	8.7 ± 0.11 (6)	5.8 ± 0.08 (6)	<5.0 (2)
3	7.0 ± 0.09 (6)	8.7 ± 0.15 (6)	8.8 ± 0.12 (6)	6.4 ± 0.10 (6)	5.9 ± 0.07 (20)[b]

[a]The pIC$_{50}$ is the negative log of the IC$_{50}$. Data are reported as the mean values ± SEM (standard error of the mean). The number in brackets refers to the number of test occasions. See the Supporting Information for assay experimental protocols. Cell adhesion data in this assay of standard compounds are described in references 12 and 22. [b]Tested <5.0 on one occasion.

Docking of 3 into an αvβ6 crystal structure: To generate binding poses, compounds were docked into αvβx X-ray crystal structures using Glide[25,26,27] (Schrödinger).

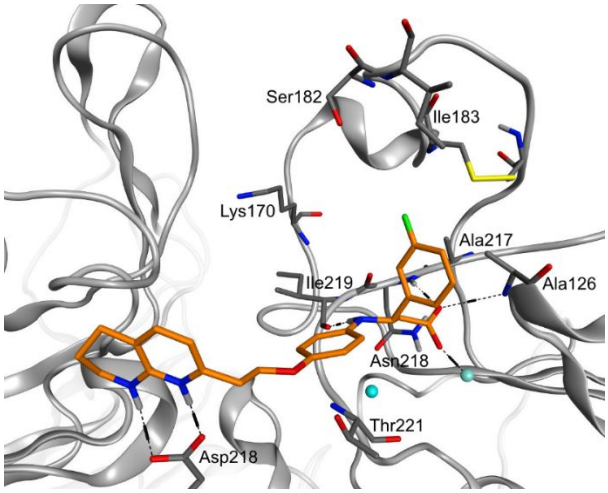

Figure 2. Docking of **3** into a crystal structure of αvβ6 (PDB code:4UM9) – see text for commentary. The left-hand part of the figure is the αv subunit and the right-hand part the β subunit.

The docked pose of **3** in an αvβ6 X-ray crystal structure (PDB code:4UM9[28]) (Figure 2) shows a bidentate H-bond between the 1,8-tetrahydronaphthyridine and αv-Asp218. In the β-subunit, the carboxylic acid motif is coordinated with the magnesium ion (cyan sphere) in the metal ion dependent adhesion site (MIDAS) and forms H-bonds with Ala126 and Asn218. The aniline NH forms a H-bond with Ile219 backbone and the *meta*-substituted aryl group is positioned in proximity to the specificity determining loop (the top right quadrant of the figure).

Synthesis: The antagonists from the phenylaminopropanoate templates were prepared using the following synthetic routes. The first route involved an SNAr reaction between a heteroaromatic core (**5**) with the tetrahydronaphthyridine ethyl alcohol (**4**) (general procedure A in SI). This was followed by a Buchwald-Hartwig coupling reaction between the aryl halide product (**6**) and phenyl azetidin-2-one (**7**) under palladium catalysed conditions. The resulting lactam ring (**8**) was then opened with aqueous lithium hydroxide to afford the desired product (**9**) in three steps (Scheme 1).

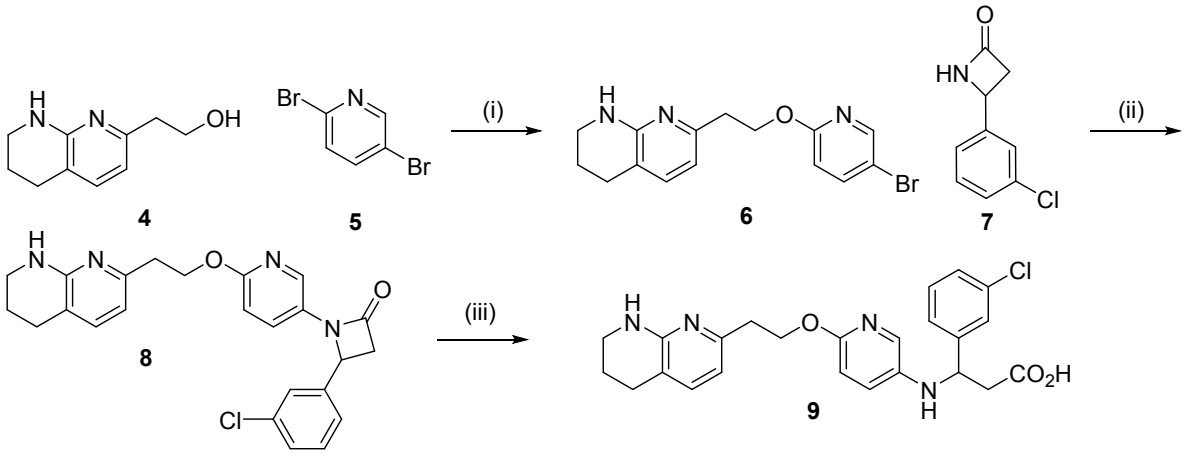

Scheme 1. General Procedure A: Reagents and conditions: (i) NaH, DMF, 0 °C (ii) PPh_3, DIAD, THF (iii) Cs_2CO_3, Xantphos, $Pd_2(dba)_3$, 1,4-dioxane, 130 °C (iv) 1M LiOH, THF.

The second route involved a Mitsunobu reaction between the tetrahydronaphthyridine ethyl alcohol (**4**) and heteroaromatic alcohol (**10**) (procedure B). The resulting heterocycle (**11**) was then also coupled with lactam (**7**) and ring opened as before to afford the desired product (**13**) (Scheme 2).

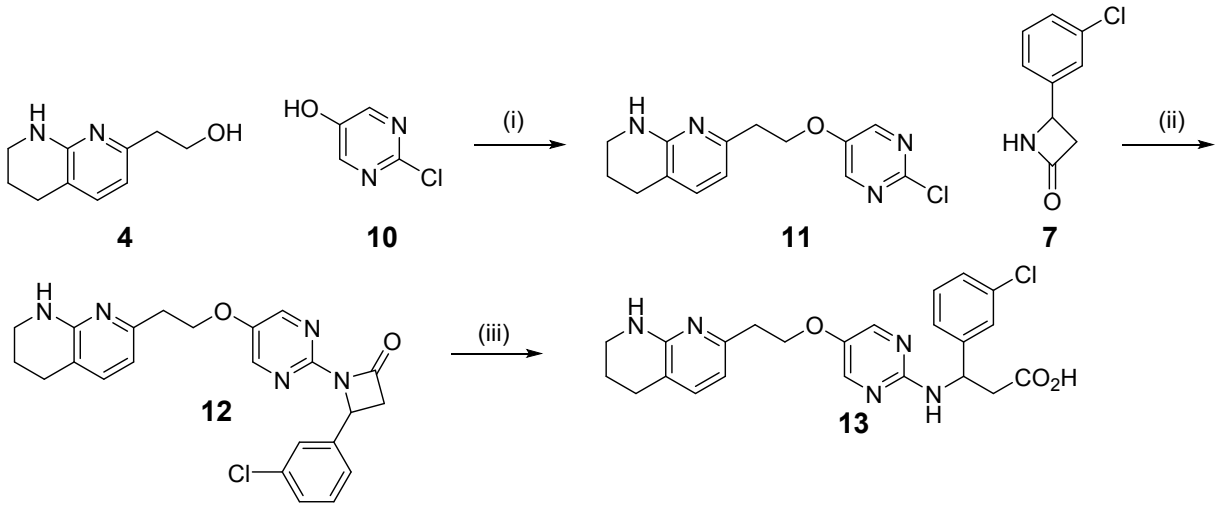

Scheme 2. General Procedure B: Reagents and conditions: (i) PPh_3, DIAD, THF (ii) Cs_2CO_3, Xantphos, $Pd_2(dba)_3$, 1,4-dioxane, 130 °C (iii) 1M LiOH, THF.

Variations to the right-hand side aromatic ring were achieved *via* an alternative synthetic route. Following a Mitsunobu reaction between the Boc protected tetrahydronaphthyridine ethyl alcohol (**14**) and 6-nitropyridin-3-ol (**15**), and subsequent reduction, the 2-amino pyridine intermediate (**16**)

was obtained. It was then refluxed to dryness in the presence of a substituted benzaldehyde (**17**) to generate the imine which was then cooled and treated with (2-(*tert*-butoxy)-2-oxoethyl)zinc(II) chloride to give the *tert*-butyl ester product (**18**) (procedure C). This fully protected compound could be deprotected in the presence of aqueous acid to afford the desired product (**19**), or further reacted in a cross-coupling reaction with a trifluoroborate salt (procedure D) or boronic acid[29] (procedure E) to give (**20**), and then deprotected to give (**21**) (Scheme 3).

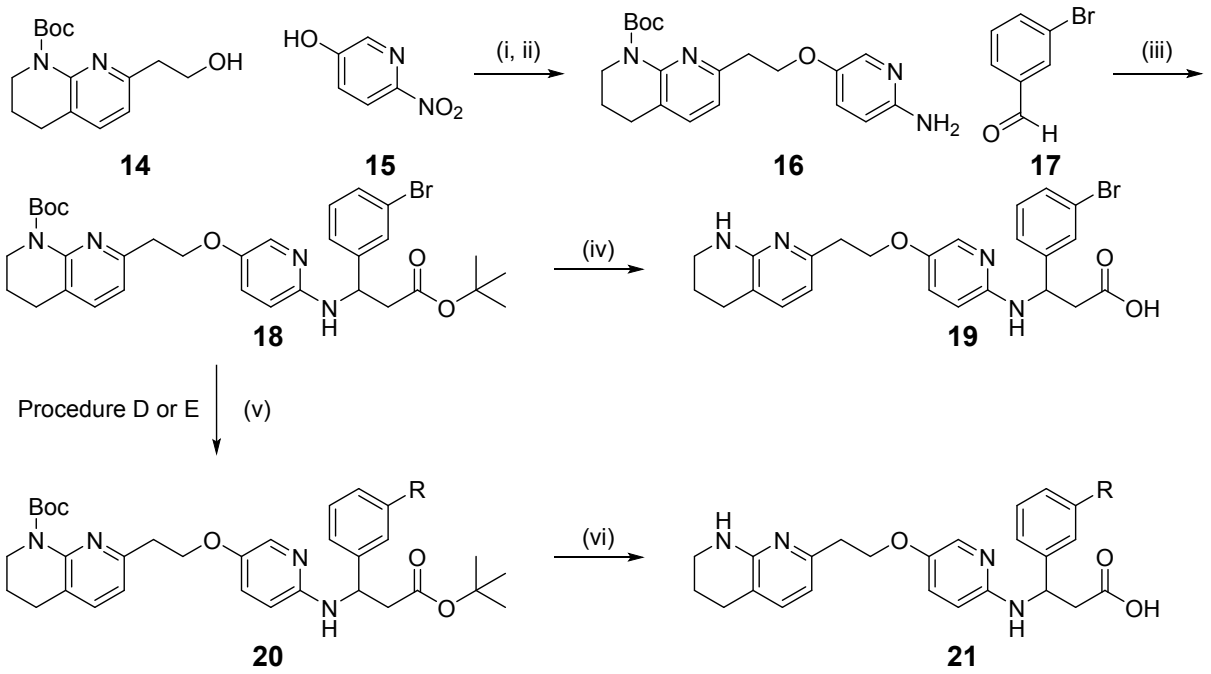

Scheme 3. General Procedure C: Reagents and conditions: (i) PPh_3, DIAD, THF (ii) Pd/C, H_2, EtOH:EtOAc (5:1) (iii) 120 ^oC, THF, then (2-(*tert*-butoxy)-2-oxoethyl)zinc(II) chloride (0.5M in THF), THF (iv) 4M HCl in 1,4-dioxane, DCM, H_2O (v) Procedure D for R-BF_3K, P(^{t}Bu)$_3$, Xphos, Cs_2CO_3, $Pd(OAc)_2$, THF, 130 ^oC. Procedure E for R-$B(OH)_2$, K_3PO_4, 2'-(dimethylamino)-2-biphenylyl-palladium(II) chloride dinorbornylphosphine complex, 1,4-dioxane, H_2O, 130 ^oC. (vi) 4M HCl in 1,4-dioxane, DCM, H_2O

Structure activity relationships – central ring modifications: The modifications of the central aromatic ring were initially investigated with a 3-Cl substituted phenyl right-hand side (R1 = Cl, Table 2) as legacy and initial SAR suggested this is a preferred group for improving αvβ6 activity. This observation was subsequently also reported in the literature on a β-phenylalanine template.[24]

Significant differences in activity and selectivity were observed for the six 6-member heteroaromatic analogues **9**, **13**, **22**-**25**. The positions of the nitrogen(s) appeared to be crucial for the αvβ6 potency, with for instance, the 5-aminopyridine **9** being nearly 10-fold less potent than the 2-aminopyridine **22** (Table 2). The 5- and 2-aminopyrimidines **23** and **13** are less effective at binding αvβ6 than the 2-aminopyridine **22**, while the aminopyrazine **25** is surprisingly nearly inactive (pIC_{50} 4.9 but 3 values out of 6 are below the 4.3 threshold of the assay). The aminopyridazine **24** is the most active antagonist of this initial set of 6 compounds. The overall selectivity profiles of these molecules are all similar, with the activities for all four αv receptors increasing or decreasing in synchrony. More specifically, these analogues are almost equipotent between αvβ6 and αvβ8 and whilst a similar effect is observed for αvβ3 and αvβ5, the inhibitory activities for the latter two integrins are typically at least 10-fold higher.[12] The superior activity of the 2-aminopyridine and aminopyridazine rings at binding to αvβ3, αvβ5, αvβ6 and αvβ8 was confirmed with the data for the 4-Cl-phenyl right hand-side analogues **26**-**31** (R2 = Cl, Table 2). Similar SAR data were observed for these antagonists although there is a trend towards slightly higher selectivity for αvβ3 and αvβ5 over αvβ6 suggesting, as one could have expected, that small modifications of the right hand-side aryl do not significantly affect the binding conformation of the central aromatic heterocycles. None of the modifications of the central aromatic ring produced more pan-like antagonists with the potencies of the molecules always remaining higher for αvβ3 and αvβ5. The increased activity of **22** and **27** for αvβ6 compared to **9** and **26** may be related to changes in the basicity of the pyridine ring – the calculated pKa's (Chemaxon) are quite different for 2-methoxy-5-methylaminopyridine (3.36) and 2-methylamino-5-methoxypyridine (5.99) and there is literature that αvβ6 inhibitors with a basic group in this region of the binding site are highly potent.[22]

Table 2. Activity and selectivity of the different aromatic central ring analogs (all compounds racemic)

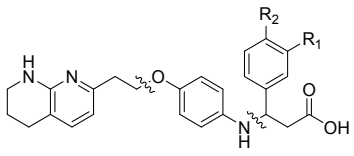

Cmpd	Core	R1	R2	pIC_{50}[a]			
				$\alpha_v\beta_6$ FP	$\alpha_v\beta_3$ FP	$\alpha_v\beta_5$ FP	$\alpha_v\beta_8$ FP
9	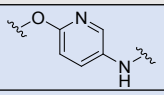	Cl	H	6.4 ± 0.26 (6)	7.9 ± 0.31 (6)	7.8 ± 0.36 (6)	6.0 ± 0.33 (6)
22	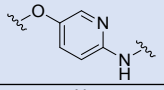	Cl	H	7.3 ± 0.04 (4)	8.2 ± 0.17 (4)	8.2 ± 0.08 (4)	7.1 ± 0.12 (4)
23	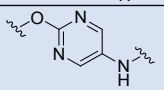	Cl	H	6.2 ± 0.47 (6)	7.3 ± 0.50 (6)	7.3 ± 0.45 (6)	5.6 ± 0.51 (6)
13	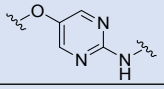	Cl	H	6.8 ± 0.07 (6)	8.3 ± 0.07 (6)	8.3 ± 0.07 (6)	6.6 ± 0.13 (6)
24	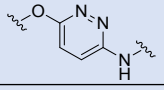	Cl	H	7.7 ± 0.04 (5)[b]	8.5 ± 0.04 (5)[b]	8.5 ± 0.11 (5)[b]	7.6 ± 0.08 (5)[b]
25	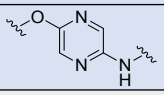	Cl	H	4.9 ± 0.07 (6)[c]	5.3 ± 0.27 (5)	5.3 ± 0.22 (6)	4.9 ± 0.05 (3)[c]
26	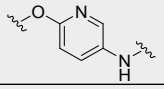	H	Cl	6.0 ± 0.28 (6)	7.4 ± 0.39 (6)	7.3 ± 0.41 (6)	5.6 ± 0.22 (6)
27	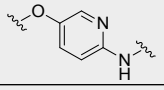	H	Cl	7.4 ± 0.11 (6)	8.5 ± 0.09 (6)	8.4 ± 0.10 (6)	6.9 ± 0.10 (6)
28	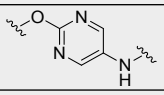	H	Cl	6.6 ± 0.27 (3)	8.1 ± 0.13 (3)	8.2 ± 0.03 (3)	6.1 ± 0.07 (3)
29	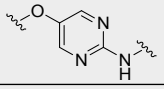	H	Cl	6.9 ± 0.23 (3)	8.9 ± 0.18 (3)	9.0 ± 0.08 (3)	7.2 ± 0.11 (3)
30	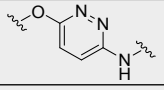	H	Cl	7.6 ± 0.05 (6)	8.7 ± 0.11 (6)	8.5 ± 0.09 (6)	7.5 ± 0.08 (6)
31	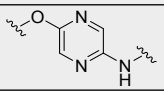	H	Cl	4.7 (1)[d]	4.9 ± 0.22 (7)[b]	4.9 ± 0.15 (7)[b]	4.5 (1)[d]

[a]See the general footnotes in Table 1. [b]Tested <4.08 on one occasion. [c]Tested <4.3 on 3 occasions. [d]Tested <4.3 on 7 occasions.

Structure activity relationships – the preferred stereochemistry: The enantiomers of the most potent analogue, the aminopyridazine **24** (referred to as **32** and **33** and depicted in Table 3) were obtained by chiral HPLC separation of the racemic mixture.[§] A small molecule crystal structure was obtained for a DMSO solvate of single enantiomer **32**.[§§] The study showed the molecule to exist as a zwitterion, with the absolute configuration unambiguously determined [(R)- at the C3 benzylic position (Figure 3)].

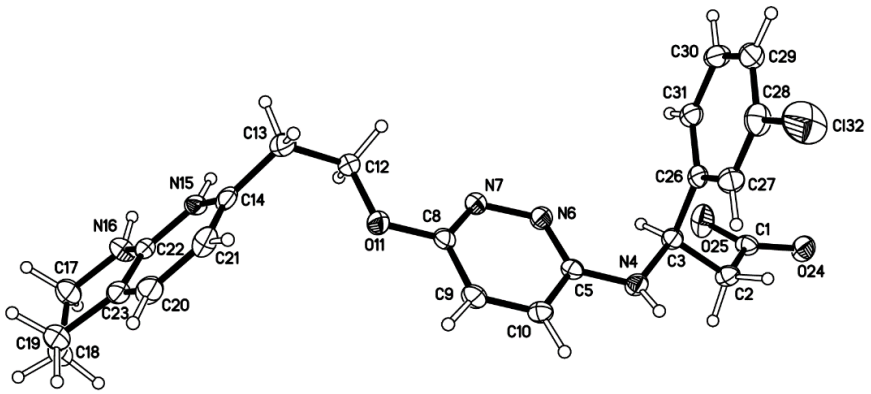

Figure 3. A molecule of **32** from its DMSO solvate crystal structure. Anisotropic atomic displacement ellipsoids for the non-hydrogen atoms are shown at the 50% probability level. Hydrogen atoms are displayed with an arbitrarily small radius.

§ The chiral separation method is 40% EtOH/heptane with a flow-rate = 1 mL/min on a column 4.6mm id x 25 cm Chiralcel OJ monitoring at a wavelength of 230 nm. Isomer 1 (**32**) eluted ca 10.5 min and isomer 2 (**33**) ca 18 min.

§§ Crystal data and refinement summary for **32** (CCDC 1919504): $C_{23}H_{24}ClN_5O_3 \cdot C_2H_6OS$; M = 532.05; colourless plate from the slow evaporation of a solution of **32** in DMSO; 0.74 x 0.50 x 0.03 mm; monoclinic; space group P21 (#4); a = 9.3008(3), b = 8.5375(2), c = 16.9166(5) Å, β = 104.657(3) °, V = 1299.56(6) Å3; T = 150(2) K; Z = 2; Dcalc = 1.360 Mgm-3; λ = 0.71073 Å; θmax = 28.57 °; reflections collected = 14493; independent reflections = 5493; Rint = 0.0267; S = 1.041; R1 [I>2σ(I)] = 0.0306; wR2 (all data) = 0.0752; Flack = 0.01(5).

The (*S*) enantiomer **33** is the more active configuration to bind to αvβ6 (pIC_{50} 8.2, Table 3) and considering the high sequence homology between αvβ6, αvβ3, αvβ5 and αvβ8, it is not surprising to observe that it is the more active enantiomer against all four integrin receptors. These data are in agreement with previous reports in the literature on β-phenylalanine or phenylbutyrate templates, which also disclosed the (*S*) configuration as the more active enantiomer,[23,24,30] suggesting that all these antagonists bind the β subunits with similar conformations.

Table 3: Data for the enantiomers of **24** confirming that the (*S*) configuration is preferred for binding to the αv integrin receptors.

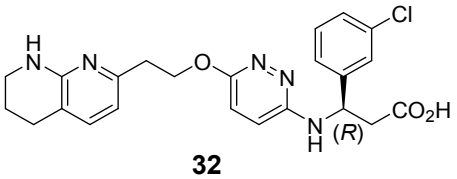

32

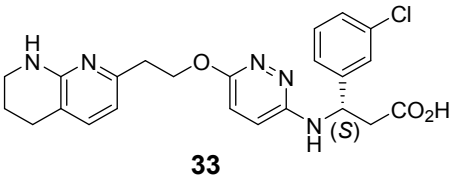

33

Cmpd	pIC_{50}[a]			
	$\alpha_v\beta6$ FP	$\alpha_v\beta3$ FP	$\alpha_v\beta5$ FP	$\alpha_v\beta8$ FP
32	6.1 ± 0.03 (5)	6.8 ± 0.02 (5)	7.9 ± 0.03 (5)	5.7 ± 0.04 (5)
33	8.2 ± 0.09 (5)	9.1 ± 0.06 (5)	8.9 ± 0.07 (5)	8.1 ± 0.07 (5)

Structure activity relationships – right hand ring substitution: To improve the overall pan αv profile, substitutions of the right-hand aryl ring were next investigated. This ring binds in the specificity determining loop of the β subunit where there are differences in the amino-acid residues between the αv integrins. From Table 2 the *meta*-chloro 2-aminopyridine **22** and aminopyridazine **24** are the most potent analogues across the integrins (alongside their *para*-chloro comparators **27** and **30**). The pyridine **22** has higher permeability through an artificial membrane (see the Supporting Information for experimental details) than the pyridazine **24** (33 nm/s and 8.4 nm/s, respectively), which may reflect its slightly higher lipophilicity (chrom logD $pH_{7.4}$ 2.74 and 2.50 for **22** and **24** respectively).[22] This, together with the increased tractability of pyridines and their greater occurrence in drugs led us to focus on exploring the right hand-side aryl ring with the 2-aminopyridine core to identify more pan like profiles and establish the suitability of the template for oral bioavailability.

The data for **22** and **27** indicate that *meta*- and *para*-chloro substitution does not significantly affect the activity and selectivity profiles. Reducing the size of the halogen (*m*-F analogue **34**, Table 4) in comparison to the chloro analogue **22** marginally reduces the αvβ6 and αvβ8 binding potencies, while the αvβ3 activity increases slightly and αvβ5 remains unchanged. It is interesting to note that although

the activity changes are minimal, this exact SAR profile has already been reported by Macdonald *et al*. in their investigation of the substitution of the aryl ring of the β-phenylalanine motif.[24] Increasing the size of the halogen (*m*-Br analogue **19**, Table 4) did not significantly alter the integrin activities compared to the **22** and neither does the *para* substitution with the electron withdrawing trifluoromethyl group (analogue **35**). The trifluoromethyl **35** data contrast with those reported for the same analogue on the β-phenylalanine motif[24] where it slightly decreases the αvβ3 and αvβ5 activities to produce an unambiguous pan αv antagonist. The *para* phenoxy substituent **36** increases the αvβ6 potency over the *para* chloro substituent **27** (albeit at the expense of increased molecular weight and lipophilicity) but the *meta* or *para* methyl morpholines **37** and **38** respectively do not systematically improve the αvβ6 potency nor significantly change the selectivity profile. In contrast, the smaller *m*-cyclopropyl analogue **39** has the best pan-like profile between the αv isoforms driven by increased activity at the αvβ6 receptor (pIC_{50} = 7.8). The 3,5-bis-cyclopropyl substitution of the aryl ring is however detrimental for the binding affinities at the receptors (**40**). This ring binds into the specificity determining loop where subtle structural changes through variation in the substituents are known to alter binding to the different αv integrins.[22,24]

Table 4. Activity and selectivity of aryl substituted analogues of **22** and **27** (all compounds racemic)

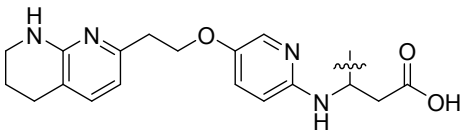

Compound	Aryl Group	pIC_{50}[a]			
		$\alpha_v\beta_6$ FP	$\alpha_v\beta_3$ FP	$\alpha_v\beta_5$ FP	$\alpha_v\beta_8$ FP
34		7.1 ± 0.06 (6)	8.6 ± 0.08 (6)	8.4 ± 0.08 (6)	6.8 ± 0.07 (6)
19		7.5 ± 0.10 (3)	8.3 ± 0.23 (3)	8.4 ± 0.08 (3)	7.2 ± 0.16 (3)
35	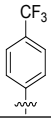	7.1 ± 0.13 (3)	8.1 ± 0.27 (3)	8.1 ± 0.20 (3)	6.7 ± 0.22 (3)

36	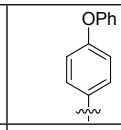	7.9 ± 0.07 (6)	8.7 ± 0.09 (6)	8.5 ± 0.11 (6)	7.1 ± 0.14 (6)
37	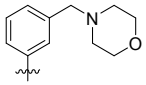	7.2 ± 0.23 (3)	8.4 ± 0.13 (3)	8.5 ± 0.05 (3)	7.2 ± 0.05 (3)
38	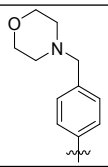	7.5 ± 0.04 (6)	8.5 ± 0.08 (6)	8.2 ± 0.07 (6)	6.9 ± 0.08 (6)
39	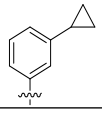	7.8 ± 0.09 (4)	8.4 ± 0.11 (4)	8.4 ± 0.10 (4)	7.4 ± 0.11 (4)
40	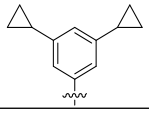	6.5 ± 0.51 (3)	6.9 ± 0.40 (3)	7.0 ± 0.49 (3)	6.9 ± 0.72 (3)

[a]See the general footnotes in Table 1.

Overall, **39** has the best profile for a pan αv antagonist from this series of compounds being more pan-like and with better physicochemical properties than **36**. The increase in activity for the αvβ6 receptor compared to the original lead **2** (Table 1) was confirmed in a αvβ6 cell adhesion assay, with **39** having a pIC_{50} of 6.9 ± 0.2 (6) (tested <5.0 on one occasion).

Docking of 39 into αvβ6 and αvβ3 crystal structures: Similarly to as described above, **39** was docked into the crystal structures of αvβ6 and αvβ3 (alongside **3** for the latter for comparison). The ligand interactions of **39** in the binding site of αvβ6 (Figure 4) are essentially as described for **3** except for the *meta*-substituted cyclopropyl group on the aryl ring which is close to lipophilic residues (Ile183, Ala217) of the specificity determining loop (the top right quadrant of the figure).

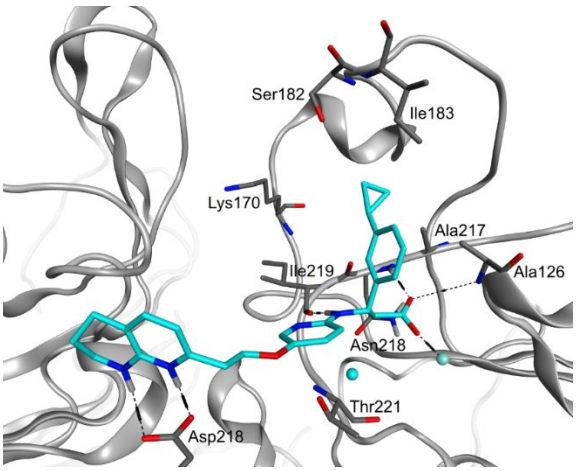

Figure 4. Docking of **39** into a crystal structure of αvβ6 (PDB code:4UM9) – see text for commentary.

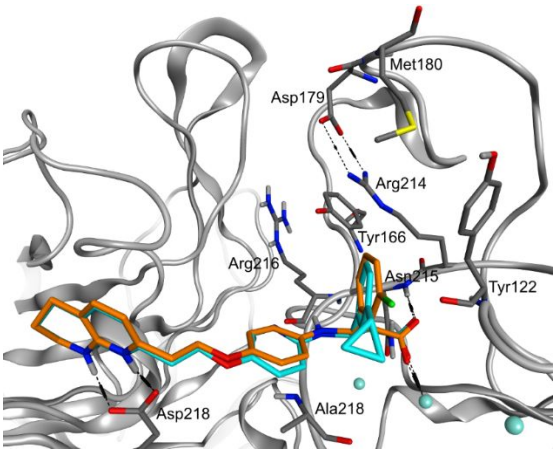

Figure 5. The binding modes of **3** (orange) and **39** (cyan) docked into an αvβ3 X-ray crystal structure (PDB code:1L5G) See text for commentary.

The predicted binding modes of **3** (orange) and **39** (cyan) in an αvβ3 X-ray crystal structure (PDB code:1L5G[31]) are shown in Figure 5. For both ligands, H-bonds between the 1,8-tetrahydronaphthyridine and αv-Asp218, and acid coordination with a manganese ion of the MIDAS and H-bond with Asn215 backbone are consistent. Due to the salt-bridge between Asp179 and Arg214, the *meta*-substituted fluoro and cyclopropyl groups on the aryl ring are directed away from these larger side-chain residues due to the reduction in the β-subunit binding site size (compared with αvβ6).

Oral pharmacokinetics The artificial membrane permeability of **39** is 80 nm/s, suggesting that it had the potential to be absorbed following oral administration. In fact, *in vivo* pharmacokinetic studies[32] in CD rats revealed that racemic **39** has a low plasma clearance of 8 mL/min/kg, a low to moderate volume of distribution of 0.5 L/kg, a moderate half-life of 1.8 h and very high bioavailability of 98% (Table 5). These pharmacokinetic data are similar to that reported for the lead compound **1** from the phenylbutyrate template,[23] indicating that the improvement in αvβ6 and αvβ8 activities obtained by modifying the central aromatic ring and the substitution of the right hand-side aryl have not been obtained at the expense of good oral profile.

Table 5. Rat pharmacokinetic data for **39**[a]

Cmpd	Cl (mL/min/kg)	Vss (L/kg)	$T_{1/2}$ (h)	Oral F (%)
39	8	0.5	1.8	98

[a]See reference 22 for typical experimental details.

Conclusion

In conclusion, we have described how small structural changes on a phenylbutyrate template - mainly based on the aromatic central core - affect the activity and selectivity for the αvβ3, αvβ5, αvβ6 and αvβ8 integrin receptors. With the aim of targeting a pan αv profile for the treatment of IPF, we have improved the αvβ6 and αvβ8 activities at these receptors by ~100 fold compared with **2**, without compromising on the good oral pharmacokinetic profile. Indeed, the new lead compound **39** from this series possess binding activities at all four integrin receptors between 4 and 40 nM as well as low clearance and an excellent bioavailability (98 %) in rats. Although our target here is IPF, a pan αv antagonist has already been reported[18] as being efficacious in a number of models of fibrotic diseases. Nevertheless, current studies are aimed at improving the overall profile and the results of our investigations in this new area will be reported in due course.

EXPERIMENTAL SECTION

Assays:

Artificial membrane permeability assay

This technique measures the permeability of a compound in a phospholipid bilayer system. The lipid is egg phosphatidyl choline (1.8%) and cholesterol (1%) dissolved in n-decane. This is applied to the bottom of the microfiltration filter inserts in a Transwell plate. Phosphate buffer (50 mM Na_2HPO_4 with 0.5% 2-hydroxypropyl-b-cyclodextrin), pH 7.4 is added to the top and bottom of the plate. The lipids are allowed to form bilayers across the small holes in the filter. Permeation experiment is

initiated by adding the compound to the bottom well and stopped at a pre-determined elapsed time. The compound permeates through the membrane to enter the acceptor well. The compound concentration in both the donor and acceptor compartments is determined by liquid chromatography after 3 hours incubation at room temperature. The permeability (logPapp) measuring how fast molecules pass through the black lipid membrane is expressed in nm/s. See Veber D.F.; Johnson S.R.; Chen H-Y.; Smith B. R.; Ward K. W.; Kopple D. Molecular properties that influence the oral bioavailability of drug candidates, *J. Med. Chem.* **2002**, *45*, 2615-2623; and Kansy M, Senner F, Gubernator K. Physicochemical high throughput screening: parallel artificial membrane permeation assay in the description of passive absorption processes. *J. Med. Chem*. **1998**, *41*, 1007–1010.

Fluoresence polarization assays

All purified soluble protein preparations (recombinantly derived from Chinese Hamster Ovary cells) for the human αvβ1, αvβ3, αvβ5, αvβ6 and αvβ8 integrin proteins used in fluorescence polarization (FP) assays were purchased from R&D Systems Inc. (Minneapolis, MN, USA). Briefly, FP assays were performed in low volume 384-well plates (Greiner Bio-One, Firckenhausen, Germany) at room temperature (20-22°C) in assay buffer (25 mM 4-(2-hydroxyethyl)-1-piperazineethanesulfonic acid, 150 mM NaCl and 1 mM 3-[(3-cholamidopropyl)dimethylammonio]-1-propanesulfonate at pH 7.4 (NaOH). Assay buffer was supplemented with 0.1 mM $MnCl_2$ for αvβ1/αvβ5/αvβ8 and 0.4 mM $MgCl_2$ for αvβ3/αvβ6. Experiments were completed in a total volume of 6.1 µL consisting of 0.1 µL/well of either compound at varying concentrations or vehicle (dimethylsulfoxide), 3 µL/well of purified integrin (final assay concentration (FAC) of 2 nM αvβ1, 1 nM αvβ3, 4 nM αvβ5 or 8 nM αvβ6/αvβ8) and 3 µL/well of **Cy3B-RGD** probe (1 nM FAC) (Fig. 6). Compounds were pre-incubated with integrin protein for 15 mins prior to addition of **Cy3B-RGD** probe. FP was then measured using an EnVision multilabel plate reader (PerkinElmer LAS UK Ltd., Beaconsfield, UK) following a further 2 h incubation.

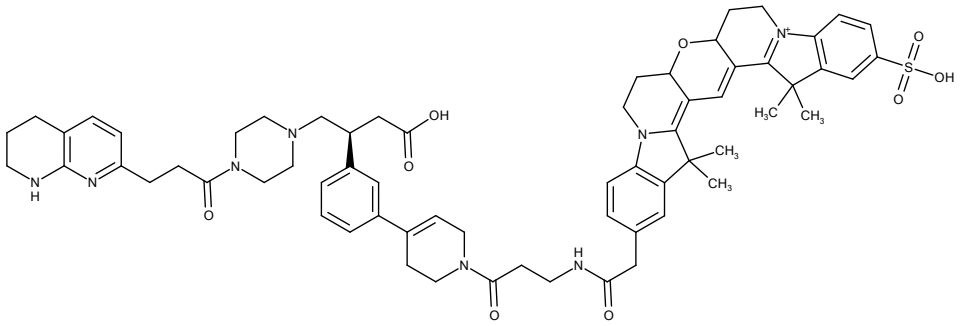

Figure 6: Cy3B-RGD probe used in fluorescence polarization experiments.

In-vivo rat pharmacokinetics

The intravenous pharmacokinetics of **39** was investigated in two male CD rats (BW: 288-312g) at 1 mg/kg. The compound was dissolved in DMSO:PEG200:water (5:45:50 v/v/v) at a concentration of 1 mg/mL and dosed as a bolus via the femoral vein. Blood samples were collected in heparinised tubes up to 7h via a tail vein canula and with additional sampling up to 24h via direct tail venipuncture.

The oral pharmacokinetics of **39** was investigated in two male CD rats (BW: 303-308g) at 1 mg/kg. The compound was dissolved in 0.5% aq. Methyl cellulose containing 0.2% Tween 80 at a concentration of 0.1 mg/mL and dosed via oral gavage. Blood samples were collected up to 7h via a tail vein canula and with additional sampling up to 24h via direct tail venipuncture.

Blood samples from both arms were centrifuged to obtain plasma, which was stored frozen at -20 ^{o}C prior to analysis. Plasma samples were mixed with acetonitrile containing internal standard and centrifuged. Supernatants were evaporated to dryness under nitrogen and reconstituted in acetonitrile:water 10:90 (v/v). The concentration of **39** was determined by LC-MS/MS.

Synthetic details

General Methods: All solvents were of analytical grade, purchased from Sigma-Aldrich in anhydrous form. Unless otherwise stated, reagents were purchased from the following suppliers: Sigma-Aldrich, Lancaster, Fluorochem, TCI and used without further purification. NMR Spectroscopy: ^{1}H NMR and ^{13}C NMR spectra were recorded on Bruker DPX-400 spectrometers at either 500, 400 or 100 MHz.

Chemical shifts (δ) are reported in parts per million (ppm) and referenced to the residual solvent peak. Coupling constants (J) are measured in hertz (Hz). Advanced experiments were recorded on an AVC-600 spectrometer and were obtained by Sean Lynn or Stephen Richards of the Analytical Chemistry Department, GlaxoSmithKline, Stevenage. Mass Spectrometry: High resolution mass spectra (HRMS) were recorded on a Micromass Autospec 500 OAT spectrometer. HRMS was recorded by Bill Leavens, Analytical Chemistry Department, GlaxoSmithKline, Stevenage. Mass spectra (LC-MS) were recorded using one of five methods:

1) Acq~2min_TFA:

TFA Generic Analytical UPLC Open Access LC/MS 2 Minute Method. The UPLC analysis was conducted on an Acquity UPLC BEH C18 column (50 mm x 2.1 mm i.d. 1.7 µm packing diameter) at 40 °C. The solvents employed were: A = 0.1% trifluoroacetic acid in H2O, B 0.1% trifluoroacetic acid in MeCN.

2) Acq~2min_For

Formic Acid Generic Analytical UPLC Open Access LC/MS 2 Minute Method. The UPLC analysis was conducted on an Acquity UPLC BEH C18 column (50 mm x 2.1 mm i.d. 1.7 µm packing diameter) at 40 °C. The solvents employed were: A = 0.1% v/v solution of formic acid in H2O, B = 0.1% v/v solution of formic acid in MeCN.

3) XBR~5min_HpH

High pH Generic Analytical HPLC Open Access LC/MS 5 Minute Method. The HPLC analysis was conducted on an XBridge C18 column (50 mm x 4.6 mm i.d. 3.5 µm packing diameter) at 30 °C. The solvents employed were: A = 10 mM ammonium bicarbonate in water adjusted to pH 10 with ammonia solution, B = Acetonitrile.

4) Sun~5min_For

Formic Acid Generic Analytical HPLC Open Access LC/MS 5 Minute Method. The HPLC analysis was conducted on an Sunfire C18 column (50 mm x 4.6 mm i.d. 3.5 µm packing diameter) at 30 °C. The

solvents employed were: A = 0.1% v/v solution of formic acid in H2O, B = 0.1% v/v solution of formic acid in MeCN.

5) Sun~5min_TFA

TFA Generic Analytical HPLC Open Access LC/MS 5 Minute Method. The HPLC analysis was conducted on an Sunfire C18 column (50 mm x 4.6 mm i.d. 3.5 µm packing diameter) at 30 °C. The solvents employed were: A = 0.1% trifluoroacetic acid in H2O, B 0.1% trifluoroacetic acid in MeCN.

Synthetic procedures

All compounds ≥ 95% purity by LC-MS and ^{1}H NMR unless otherwise stated.

General procedure A: SNAr, Buchwald-Hartwig cross coupling, hydrolysis

7-(2-((5-Bromopyridin-2-yl)oxy)ethyl)-1,2,3,4-tetrahydro-1,8-naphthyridine (6) To a stirred solution of 2-(5,6,7,8-tetrahydro-1,8-naphthyridin-2-yl)ethanol (300 mg, 1.683 mmol) in DMF (5 mL) at 0 °C and under N_2 was added NaH (60% dispersion in mineral oil, 81 mg, 2.020 mmol) and the reaction mixture was stirred at 0 °C for 30 mins. The reaction mixture was warmed to rt and 2,5-dibromopyridine (478 mg, 2.020 mmol) was added. The reaction mixture was then stirred at rt and under N_2 for a further 19 h. Further NaH (60% dispersion in mineral oil, 81 mg, 2.020 mmol) was added and the reaction mixture stirred for a further 4 h. The reaction mixture was partitioned between DCM (15 ml) and H_2O (15 mL) the layers were separated and the aq. layer washed with further DCM (15 mL). The combined organic phases were dried by passing through a hydrophobic frit and concentrated *in vacuo* to afford the crude product as a brown solid. The sample was purified by silica chromatography, eluting with EtOAc:cyclohexane (0 - 100% EtOAc). The appropriate fractions were combined and concentrated in vacuo to give the title compound (314 mg, 56%) as a white solid. ^{1}H NMR (400 MHz, DMSO) δ ppm = 8.27 (d, J=2.5 Hz, 1H), 7.87 (dd, J=2.8, 8.8 Hz, 1H), 7.05 (d, J=7.3 Hz, 1H), 6.78 (d, J=8.8 Hz, 1H), 6.36 - 6.31 (m, 2H), 4.50 (t, J=6.9 Hz, 2H), 3.27 - 3.20 (m, 2H), 2.88 (t, J=6.9

Hz, 2H), 2.61 (t, J=6.3 Hz, 2H), 1.75 (quin, J=5.9 Hz, 2H). LC-MS (Acq~2min_For) tR = 0.80 min, [M+H$^+$] = 334/336.

3-(3-Chlorophenyl)-3-((6-(2-(5,6,7,8-tetrahydro-1,8-naphthyridin-2-yl)ethoxy)pyridin-3-yl)amino)propanoic acid (9) A solution of 7-{2-[(5-bromo-2-pyridinyl)oxy]ethyl}-1,2,3,4-tetrahydro-1,8-naphthyridine (100 mg, 0.299 mmol), 4-(3-chlorophenyl)-2-azetidinone (65.2 mg, 0.359 mmol), Cs_2CO_3 (292 mg, 0.898 mmol), Xantphos (17.31 mg, 0.030 mmol) and $Pd_2(dba)_3$ (13.70 mg, 0.015 mmol) in 1,4-Dioxane (5 mL) was heated in a Biotage Initiator microwave at 130 °C for 30 min. The reaction mixture was partitioned between DCM (15 mL) and H_2O (15 mL), the layers were separated and the aq. layer washed with further DCM (15 ml). The combined organic phases were then dried through a hydrophobic frit and concentrated *in vacuo* to afford a yellow oil. The sample was dissolved in THF (3 mL) and 1M aq. LiOH (3 mL, 3.00 mmol) was added. The reaction mixture was stirred at rt for 16 h. The reaction mixture was then concentrated *in vacuo* before being dissolved in MeOH:DMSO (1:1, 1 mL) and purified by mass directed autoprep on Sunfire C18 column using MeCN:H_2O with a formic acid modifier. The solvent was dried under a stream of N_2 in the Radleys blowdown apparatus to give the title compound (43 mg, 32%) as an orange solid. ^{1}H NMR (400 MHz, DMSO) δ ppm = 7.50 (s, 1H), 7.42 - 7.37 (m, 2H), 7.32 (t, J=7.8 Hz, 1H), 7.27 - 7.23 (m, 1H), 7.04 - 6.99 (m, 2H), 6.49 (d, J=8.8 Hz, 1H), 6.34 - 6.31 (m, 1H), 6.29 (d, J=7.3 Hz, 1H), 6.05 (br. s., 1H), 4.74 (t, J=6.7 Hz, 1H), 4.31 (t, J=6.9 Hz, 2H), 3.25 - 3.19 (m, 3H), 2.79 (t, J=6.9 Hz, 2H), 2.75 - 2.56 (m, 4H), 1.78 - 1.70 (m, 2H). LC-MS (Acq~2min_For) tR = 0.79 min, [M+H$^+$] = 453.

General procedure B: Mitsunobo, Buchwald-Hartwig cross coupling, hydrolysis

7-(2-((2-chloropyrimidin-5-yl)oxy)ethyl)-1,2,3,4-tetrahydro-1,8-naphthyridine (11) To a solution of 2-chloro-5-pyrimidinol (1.266 g, 9.70 mmol) and 2-(5,6,7,8-Tetrahydro-1,8-naphthyridin-2-yl)ethan-1-ol (1.73 g, 9.70 mmol) in THF (5 mL) at 0 °C and under N_2 was added triphenylphosphine (2.54 g, 9.70 mmol) and DIAD (1.886 mL, 9.70 mmol) and the reaction mixture stirred for 18 h during which time it warmed to rt. The reaction was then partitioned between DCM (100 mL) and H_2O (100 mL), the aq.

phase was washed with further DCM (100 mL) and the combined organics concentrated *in vacuo* to give the crude product. This was purified by silica chromatography, eluting with EtOAc:cyclohexane (0 - 100% EtOAc), then MeOH in DCM (0 - 15% MeOH). The appropriate fractions were concentrated *in vacuo* to give the target compound (680 mg, 24%). ^{1}H NMR (400 MHz, CDCl3) δ ppm = 8.32 (s, 2H), 7.30 (d, J=7.3 Hz, 1H), 7.25 (br. s., 1H), 6.49 (d, J=7.3 Hz, 1H), 4.50 (t, J=6.1 Hz, 2H), 3.52 - 3.46 (m, 2H), 3.19 (t, J=6.1 Hz, 2H), 2.76 (t, J=6.1 Hz, 2H), 2.00 - 1.90 (m, 2H). LC-MS (Acq~2min_For) tR = 0.59 min, [M+H$^+$] = 291

3-(3-chlorophenyl)-3-((5-(2-(5,6,7,8-tetrahydro-1,8-naphthyridin-2-yl)ethoxy)pyrimidin-2-yl)amino)propanoic acid (13) In a microwave vial was 7-{2-[(2-chloro-5-pyrimidinyl)oxy]ethyl}-1,2,3,4-tetrahydro-1,8-naphthyridine (100 mg, 0.344 mmol), 4-(3-chlorophenyl)-2-azetidinone (75.0 mg, 0.413 mmol), $Pd_2(dba)_3$ (15.75 mg, 0.017 mmol), cesium carbonate (336 mg, 1.032 mmol) and Xantphos (19.90 mg, 0.034 mmol) in 1,4-Dioxane (5 mL) and the reaction mixture was heated to 130 °C for 30 min. The reaction mixture was then partitioned between DCM (20 mL) and H_2O (20 mL), the aq. phase was separated and washed with further DCM (20 mL). The combined organic phases were then concentrated *in vacuo* to give an orange gum. This was dissolved in THF:H_2O (6 mL, 1:1) and aq. lithium hydroxide (3 mL, 3.00 mmol) was added and the mixture stirred at 20 °C for 72 h. The reaction mixture was then concentrated *in vacuo* and purified by mass directed autoprep on Sunfire C18 column using MeCN:H_2O with a TFA modifier. The solvent was dried under a stream of N_2 in the Radleys blowdown apparatus to give the title compound (5.7 mg, 4%) as a yellow gum. ^{1}H NMR (400 MHz, MeOD) δ ppm = 8.07 (s, 2H), 7.61 (d, J=7.3 Hz, 1H), 7.44 - 7.42 (m, 1H), 7.37 - 7.33 (m, 1H), 7.29 (t, J=7.7 Hz, 1H), 7.25 - 7.20 (m, 1H), 6.74 (d, J=7.5 Hz, 1H), 5.40 (dd, J=6.0, 8.0 Hz, 1H), 4.27 (t, J=6.0 Hz, 2H), 3.54 - 3.49 (m, 2H), 3.13 (t, J=6.0 Hz, 2H), 2.95 - 2.77 (m, 4H), 2.00 - 1.92 (m, 2H). two exchangeable protons not observed. LC-MS (XBR~5min_HpH) tR = 2.14 min, [M+H$^+$] = 454

General procedure C: Mitsunobu, reduction, condensation, organo zinc addition, hydrolysis

Tert-butyl 7-(2-((6-aminopyridin-3-yl)oxy)ethyl)-3,4-dihydro-1,8-naphthyridine-1(2H)-carboxylate (16) To a solution of 6-nitro-3-pyridinol (2g, 14.28 mmol) and 1,1-dimethylethyl 7-(2-hydroxyethyl)-3,4-dihydro-1,8-naphthyridine-1(2H)-carboxylate (3.97 g, 14.28 mmol) in THF (50 mL) under N_2 at 0 °C was added DIAD (4.16 mL, 21.41 mmol) and triphenylphosphine (5.62 g, 21.41 mmol) and the reaction mixture was stirred for 18 h. The reaction mixture was then concentrated *in vacuo* and partitioned between DCM (100 mL) and H_2O (100 mL). The aq. phase was washed with further DCM (100 mL) and the combined organics were concentrated *in vacuo* and purified by silica chromatography, eluting with EtOAc:cyclohexane (0 – 60 % EtOAc). The appropriate fractions were concentrated *in vacuo* to give a yellow soild. The solid was dissolved in EtOH (100 mL) and EtOAc (20 mL), 10% Pd/C (1.519g, 1.428 mmol) was added and the reaction mixture stirred under an atmosphere of H_2 for 18 h. The reaction was then filtered through celite and concentrated *in vacuo* to give an orange oil. The oil was then purified by silica chromatography, eluting with EtOAc:cyclohexane (0 – 100 % EtOAc) then with DCM:MeOH (0 - 25% MeOH). The appropriate fractions were concentrated *in vacuo* to give the target compound (2.1 g, 40%) as a yellow oil. ^{1}H NMR (400 MHz, DMSO) δ ppm = 7.62 (d, J=3.0 Hz, 1H), 7.44 (d, J=7.5 Hz, 1H), 7.09 (dd, J=3.0, 8.8 Hz, 1H), 6.99 (d, J=7.5 Hz, 1H), 6.40 (d, J=8.8 Hz, 1H), 5.44 (s, 2H), 4.23 (t, J=6.8 Hz, 2H), 3.66 - 3.61 (m, 2H), 3.02 (t, J=6.8 Hz, 2H), 2.70 (t, J=6.7 Hz, 2H), 1.82 (quin, J=6.3 Hz, 2H), 1.43 (s, 9H) LC-MS (XBR~5mins_HpH) tR = 2.52 mins, [M+H$^+$] = 371

Tert-butyl 7-(2-((6-((1-(3-bromophenyl)-3-(tert-butoxy)-3-oxopropyl)amino)pyridin-3-yl)oxy)ethyl)-3,4-dihydro-1,8-naphthyridine-1(2H)-carboxylate (18) 1,1-dimethylethyl 7-{2-[(6-amino-3-pyridinyl)oxy]ethyl}-3,4-dihydro-1,8-naphthyridine-1(2H)-carboxylate (500 mg, 1.350 mmol) and 3-bromobenzaldehyde (0.157 mL, 1.350 mmol) were dissolved in THF (5 mL) and the reaction mixture was then evaporated to dryness at 120 °C for 2 h. The reaction mixture was then cooled to rt and re-dissolved in THF (15 mL), to this was added (2-(tert-butoxy)-2-oxoethyl)zinc(II) chloride (0.5 M in THF, 8.10 mL, 4.05 mmol) and the mixture stirred at rt for 18 h. The reaction mixture was then concentrated *in vacuo* and re-dissolved in DCM (50 mL) and washed with sat. aq. NH_4Cl (50 mL), the aq. phase was separated and washed with further DCM (50 mL), the combined organic fractions were then

concentrated in vacuo and purified by silica chromatography, eluting with EtOAc:cyclohexane (0 - 50 % EtOAc), the appropriate fractions were concentrated *in vacuo* to give the target compound (650 mg, 66%) as a yellow oil. ^{1}H NMR (400 MHz, DMSO) δ ppm = 7.67 (d, J=2.8 Hz, 1H), 7.57 (s, 1H), 7.46 - 7.36 (m, 3H), 7.26 (d, J=7.5 Hz, 1H), 7.10 (dd, J=3.0, 9.0 Hz, 1H), 6.97 (d, J=7.5 Hz, 1H), 6.73 (d, J=8.8 Hz, 1H), 6.47 (d, J=8.8 Hz, 1H), 4.22 (t, J=6.8 Hz, 2H), 3.65 - 3.60 (m, 2H), 2.99 (t, J=6.7 Hz, 2H), 2.79 - 2.56 (m, 5H), 1.81 (quin, J=6.3 Hz, 2H), 1.39 (s, 9H), 1.28 (s, 9H) LCMS (XBR~5mins_HpH) tR = 3.86 mins, [M+H$^+$] = 653 / 655

3-(3-Bromophenyl)-3-((5-(2-(5,6,7,8-tetrahydro-1,8-naphthyridin-2-yl)ethoxy)pyridin-2-yl)amino)propanoic acid (19) To a solution of tert-butyl 7-(2-((6-((1-(3-bromophenyl)-3-(tert-butoxy)-3-oxopropyl)amino)pyridin-3-yl)oxy)ethyl)-3,4-dihydro-1,8-naphthyridine-1(2H)-carboxylate (44 mg, 0.067 mmol) in DCM (2 mL) was added 4M HCl in 1,4-dioxane (0.5 ml, 2.000 mmol) and two drops of H2O and the reaction mixture stirred at rt for 18 h. The reaction mixture was then concentrated *in vacuo* and dissolved in MeOH:DMSO (1:1, 1 mL) and purified by mass directed autoprep on Xbridge column using MeCN:H2O with an ammonium carbonate modifier. The solvent was dried under a stream of N2 in the Radleys blowdown apparatus to give the title compound (17.7 mg, 53%). ^{1}H NMR (400 MHz, MeOD) δ ppm = 7.62 - 7.56 (m, 2H), 7.42 - 7.37 (m, 1H), 7.36 - 7.30 (m, 1H), 7.21 (dd, J=7.7, 10.9 Hz, 2H), 7.10 (dd, J=3.0, 9.0 Hz, 1H), 6.48 (d, J=7.3 Hz, 1H), 6.42 (d, J=9.0 Hz, 1H), 5.08 (t, J=6.9 Hz, 1H), 4.14 (t, J=6.5 Hz, 2H), 3.42 - 3.35 (m, 3H), 2.94 (t, J=6.5 Hz, 2H), 2.72 (t, J=6.1 Hz, 2H), 2.67 (d, J=7.0 Hz, 2H), 1.92 - 1.85 (m, 2H). Two exchangeable protons not observed, LC-MS (XBR~5mins_HpH) tR = 2.22 mins, [M+H$^+$] = 497 / 499

3-(3-Chlorophenyl)-3-((5-(2-(5,6,7,8-tetrahydro-1,8-naphthyridin-2-yl)ethoxy)pyridin-2-yl)amino)propanoic acid (22), Prepared by general procedure C using 4-(3-chlorophenyl)azetidin-2-one. ^{1}H NMR (400 MHz, $CDCl_3$) δ ppm = 8.47 (br. s., 1H), 7.62 (br. s., 1H), 7.42 (s, 1H), 7.35 - 7.17 (m, 4H), 7.11 - 7.04 (m, 1H), 6.36 (d, J=7.3 Hz, 1H), 6.22 (d, J=9.0 Hz, 1H), 4.88 (t, J=6.4 Hz, 1H), 4.19 - 4.09 (m, 2H), 3.45 (t, J=5.0 Hz, 2H), 3.06 (t, J=5.4 Hz, 2H), 2.84 - 2.75 (m, 2H), 2.72 (t, J=6.0 Hz, 2H), 1.96 -

1.86 (m, 2H), two exchangeable protons not observed, LC-MS (XBR~5min_HpH) tR = 2.2 min, [M+H$^+$] = 453

3-(3-Chlorophenyl)-3-((2-(2-(5,6,7,8-tetrahydro-1,8-naphthyridin-2-yl)ethoxy)pyrimidin-5-yl)amino)propanoic acid (23), prepared by general procedure C using 4-(3-chlorophenyl)azetidin-2-one. ^{1}H NMR (400 MHz, DMSO) δ ppm = 7.93 (s, 2H), 7.53 - 7.51 (m, 1H), 7.42 - 7.38 (m, 1H), 7.34 (t, J=7.8 Hz, 1H), 7.29 - 7.25 (m, 1H), 7.03 (d, J=7.3 Hz, 1H), 6.34 - 6.27 (m, 2H), 4.84 - 4.76 (m, 1H), 4.37 (t, J=6.9 Hz, 2H), 3.27 - 3.17 (m, 4H), 2.81 (t, J=6.9 Hz, 2H), 2.76 - 2.64 (m, 2H), 2.60 (t, J=6.4 Hz, 2H), 1.74 (quin, J=5.9 Hz, 2H), LC-MS (Acq~2min_For) tR = 0.76 min, [M+H$^+$] = 454

3-(3-Chlorophenyl)-3-((6-(2-(5,6,7,8-tetrahydro-1,8-naphthyridin-2-yl)ethoxy)pyridazin-3-yl)amino)propanoic acid (24), prepared by general procedure C using 4-(3-chlorophenyl)azetidin-2-one. ^{1}H NMR (400 MHz, CDCl3) δ ppm = 10.58 (br. s., 1H), 8.41 (s, 1H), 7.45 - 7.41 (m, 1H), 7.35 - 7.31 (m, 1H), 7.26 - 7.21 (m, 2H), 7.19 (d, J=9.3 Hz, 1H), 6.71 - 6.65 (m, 2H), 6.34 (d, J=7.3 Hz, 1H), 5.24 (dd, J=4.4, 8.4 Hz, 1H), 4.59 - 4.46 (m, 2H), 3.44 (t, J=5.5 Hz, 2H), 3.17 - 3.03 (m, 2H), 2.86 - 2.74 (m, 2H), 2.71 (t, J=6.0 Hz, 2H), 1.94 - 1.86 (m, 2H), one exchangeable proton not observed, LC-MS (SUN~5min_For) tR = 2.14 min, [M+H$^+$] = 454

3-(3-Chlorophenyl)-3-((5-(2-(5,6,7,8-tetrahydro-1,8-naphthyridin-2-yl)ethoxy)pyrazin-2-yl)amino)propanoic acid (25), prepared by general procedure C using 4-(3-chlorophenyl)azetidin-2-one. ^{1}H NMR (400 MHz, DMSO) δ ppm = 7.47 (d, J=3.0 Hz, 1H), 7.46 (s, 1H), 7.37 - 7.25 (m, 3H), 7.24 (d, J=3.3 Hz, 1H), 7.08 - 7.02 (m, 2H), 6.42 - 6.38 (m, 2H), 5.49 - 5.42 (m, 1H), 4.55 (t, J=7.2 Hz, 2H), 3.24 (t, J=5.4 Hz, 2H), 3.01 - 2.93 (m, 3H), 2.80 (dd, J=6.0, 15.8 Hz, 1H), 2.62 (t, J=6.1 Hz, 2H), 1.75 (quin, J=5.8 Hz, 2H), one exchangeable proton not observed, under H2O peak. LC-MS (Acq~2min_For) tR = 2.14 min, [M+H$^+$] = 454

3-(4-Chlorophenyl)-3-((6-(2-(5,6,7,8-tetrahydro-1,8-naphthyridin-2-yl)ethoxy)pyridin-3-yl)amino)propanoic acid (26), prepared by general procedure C using 4-(4-chlorophenyl)azetidin-2-one. ^{1}H NMR (400 MHz, DMSO) δ ppm = 7.45 - 7.42 (m, 2H), 7.39 - 7.33 (m, 3H), 7.04 - 6.97 (m, 2H),

6.48 (d, J=8.8 Hz, 1H), 6.32 (br. s., 1H), 6.29 (d, J=7.3 Hz, 1H), 6.04 (br. s., 1H), 4.72 (t, J=6.9 Hz, 1H), 4.31 (t, J=6.9 Hz, 2H), 3.60 - 3.30 (m, 2H), 2.78 (t, J=7.0 Hz, 2H), 2.75 - 2.66 (m, 1H), 2.64 - 2.55 (m, 3H), 1.74 (quin, J=5.8 Hz, 2H), one exchangeable proton not observed, under H2O peak, LC-MS (SUN~5min_For) tR = 1.70 min, [M+H$^+$] = 453

3-(4-Chlorophenyl)-3-((5-(2-(5,6,7,8-tetrahydro-1,8-naphthyridin-2-yl)ethoxy)pyridin-2-yl)amino)propanoic acid (27), prepared by general procedure C using 4-(4-chlorophenyl)azetidin-2-one. ^{1}H NMR (400 MHz, DMSO) δ ppm = 13.58 (br. s., 1H), 12.32 (br. s., 1H), 8.04 (br. s., 1H), 7.63 (d, J=3.0 Hz, 1H), 7.61 (d, J=7.5 Hz, 1H), 7.41 (d, J=8.0 Hz, 2H), 7.36 (d, J=8.0 Hz, 2H), 7.29 (br. s., 1H), 6.70 (d, J=7.3 Hz, 1H), 6.63 - 6.67 (m, 1H), 5.19 - 5.27 (m, 1H), 4.18 (t, J=6.1 Hz, 2H), 3.40 (t, J=6.0 Hz, 2H), 3.06 (t, J=6.0 Hz, 2H), 2.78 (dd, J=16.1, 8.5 Hz, 1H), 2.73 (t, J=6.0 Hz, 2H), 2.70 (dd, J=16.0, 5.5 Hz, 1H), 1.81 (quin, J=6.0 Hz, 2H), LC-MS (Sun~5min_TFA) tR = 1.84 min, [M+H$^+$] = 453

3-(4-Chlorophenyl)-3-((2-(2-(5,6,7,8-tetrahydro-1,8-naphthyridin-2-yl)ethoxy)pyrimidin-5-yl)amino)propanoic acid (28), prepared by general procedure C using 4-(4-chlorophenyl)azetidin-2-one. ^{1}H NMR (400 MHz, $CDCl_3$) δ ppm = 10.89 (br. s., 1H), 7.95 (s, 2H), 7.37 - 7.31 (m, 2H), 7.30 - 7.21 (m, 4H), 6.47 (d, J=7.0 Hz, 1H), 4.65 - 4.51 (m, 3H), 3.42 (t, J=5.1 Hz, 2H), 3.18 - 3.12 (m, 2H), 2.77 - 2.66 (m, 3H), 2.65 - 2.54 (m, 1H), 1.93 - 1.84 (m, 2H), LC-MS (Acq~2min_For) tR = 0.71 min, [M+H$^+$] = 454

3-(4-Chlorophenyl)-3-((5-(2-(5,6,7,8-tetrahydro-1,8-naphthyridin-2-yl)ethoxy)pyrimidin-2-yl)amino)propanoic acid (29), prepared by general procedure C using 4-(4-chlorophenyl)azetidin-2-one. ^{1}H NMR (400 MHz, MeOD) δ ppm = 8.32 (s, 2H), 8.01 (s, 2H), 7.45 (d, J=7.3 Hz, 1H), 7.38 (d, J=8.3 Hz, 2H), 7.28 - 7.23 (m, 2H), 6.61 (d, J=7.3 Hz, 1H), 5.38 (t, J=7.0 Hz, 1H), 4.22 (t, J=6.0 Hz, 2H), 3.47 - 3.41 (m, 2H), 3.07 (t, J=6.1 Hz, 2H), 2.89 - 2.73 (m, 4H), 1.95 - 1.88 (m, 2H), one exchangeable proton not observed, LC-MS (SUN~5min_For) tR = 1.55 min, [M+H$^+$] = 454

3-(4-Chlorophenyl)-3-((6-(2-(5,6,7,8-tetrahydro-1,8-naphthyridin-2-yl)ethoxy)pyridazin-3-yl)amino)propanoic acid (30), prepared by general procedure C using 4-(4-chlorophenyl)azetidin-2-one. ^{1}H NMR (400 MHz, MeOD) δ ppm = 12.53 (br. s, 1H), 8.15 (s, 1H), 7.44 - 7.33 (m, 4H), 7.08 (d,

J=7.8 Hz, 1H), 7.04 (d, J=7.3 Hz, 1H), 6.93 - 6.88 (m, 1H), 6.84 - 6.80 (m, 1H), 6.37 (br. s., 1H), 6.32 (d, J=7.3 Hz, 1H), 5.35 - 5.27 (m, 1H), 4.47 (t, J=6.9 Hz, 2H), 3.63 - 3.30 (m, 1H), 2.89 - 2.76 (m, 3H), 2.71 - 2.64 (m, 1H), 2.61 (t, J=6.1 Hz, 2H), 1.74 (quin, J=5.9 Hz, 2H), LC-MS (Acq~2min_For) tR = 0.62 min, $[M+H^+]$ = 454

3-(4-Chlorophenyl)-3-((5-(2-(5,6,7,8-tetrahydro-1,8-naphthyridin-2-yl)ethoxy)pyrazin-2-yl)amino)propanoic acid (31), prepared by general procedure C using 4-(4-chlorophenyl)azetidin-2-one. ^{1}H NMR (400 MHz, DMSO) δ ppm = 7.46 (d, J=3.3 Hz, 1H), 7.43 - 7.31 (m, 4H), 7.23 (d, J=3.0 Hz, 1H), 7.06 (d, J=7.3 Hz, 1H), 6.98 (d, J=8.5 Hz, 1H), 6.39 (d, J=7.0 Hz, 2H), 5.48 - 5.41 (m, 1H), 4.54 (t, J=7.2 Hz, 2H), 3.27 - 3.22 (m, 2H), 3.01 - 2.90 (m, 4H), 2.82 - 2.74 (m, 1H), 2.62 (t, J=6.3 Hz, 2H), 1.75 (quin, J=5.8 Hz, 2H), LC-MS (Acq~2min_For) tR = 0.78 min, $[M+H^+]$ = 454

(R)-3-(3-Chlorophenyl)-3-((6-(2-(5,6,7,8-tetrahydro-1,8-naphthyridin-2-yl)ethoxy)pyridazin-3-yl)amino)propanoic acid (32), prepared by general procedure A using 4-(3-chlorophenyl)azetidin-2-one. ^{1}H NMR (400 MHz, DMSO) δ ppm = 12.32 (br. s., 1H), 7.44 (s, 1H), 7.39 - 7.31 (m, 2H), 7.30 - 7.25 (m, 1H), 7.11 (d, J=8.0 Hz, 1H), 7.04 (d, J=7.3 Hz, 1H), 6.95 - 6.89 (m, 1H), 6.86 - 6.80 (m, 1H), 6.37 (br. s., 1H), 6.32 (d, J=7.3 Hz, 1H), 5.37 - 5.28 (m, 1H), 4.48 (t, J=6.9 Hz, 2H), 3.26 - 3.20 (m, 2H), 2.86 (t, J=6.9 Hz, 2H), 2.84 - 2.67 (m, 2H), 2.61 (t, J=6.1 Hz, 2H), 1.74 (quin, J=5.8 Hz, 2H), LC-MS (XBR~5mins_HpH) tR = 2.12 mins, $[M+H^+]$ = 454

(S)-3-(3-Chlorophenyl)-3-((6-(2-(5,6,7,8-tetrahydro-1,8-naphthyridin-2-yl)ethoxy)pyridazin-3-yl)amino)propanoic acid (33), prepared by general procedure A using 4-(3-chlorophenyl)azetidin-2-one. ^{1}H NMR (400 MHz, DMSO) δ ppm = 12.29 (br. s., 1H), 7.44 (s, 1H), 7.38 - 7.31 (m, 2H), 7.30 - 7.25 (m, 1H), 7.11 (d, J=8.3 Hz, 1H), 7.04 (d, J=7.3 Hz, 1H), 6.94 - 6.90 (m, 1H), 6.85 - 6.81 (m, 1H), 6.36 (br. s., 1H), 6.32 (d, J=7.3 Hz, 1H), 5.36 - 5.28 (m, 1H), 4.48 (t, J=6.9 Hz, 2H), 3.26 - 3.20 (m, 2H), 2.86 (t, J=6.8 Hz, 2H), 2.83 - 2.66 (m, 2H), 2.61 (t, J=6.1 Hz, 2H), 1.74 (quin, J=5.8 Hz, 2H), LC-MS (XBR~5mins_HpH) tR = 2.12 mins, $[M+H^+]$ = 454.

(S)-3-(3-Fluorophenyl)-3-((5-(2-(5,6,7,8-tetrahydro-1,8-naphthyridin-2-yl)ethoxy)pyridin-2-yl)amino)propanoic acid (34), prepared by general procedure C using 4-(3-fluorophenyl)azetidin-2-one. ^{1}H NMR (400 MHz, CDCl3) δ ppm = 10.13 (br. s, 1H), 7.61 - 7.57 (m, 1H), 7.36 - 7.27 (m, 3H), 7.21 (d, J=7.8 Hz, 1H), 7.17 - 7.11 (m, 1H), 7.00 - 6.92 (m, 1H), 6.41 (d, J=7.3 Hz, 1H), 6.38 (d, J=9.5 Hz, 1H), 4.90 (dd, J=4.6, 8.9 Hz, 1H), 4.22 - 4.13 (m, 2H), 3.52 - 3.46 (m, 2H), 3.11 (t, J=5.9 Hz, 2H), 2.94 - 2.79 (m, 2H), 2.75 (t, J=6.0 Hz, 2H), 1.93 (quin, J=5.9 Hz, 2H). Two exchangeable protons not observed, LC-MS (XBR~5mins_HpH) tR = 2.11 mins, [M+H$^+$] = 437

3-((5-(2-(5,6,7,8-Tetrahydro-1,8-naphthyridin-2-yl)ethoxy)pyridin-2-yl)amino)-3-(4-(trifluoromethyl)phenyl)propanoic acid (35), prepared by general procedure C using 4-(trifluoromethyl)benzaldehyde. ^{1}H NMR (400 MHz, DMSO) δ ppm = 7.72 - 7.54 (m, 5H), 7.09 (dd, J=2.9, 8.9 Hz, 1H), 7.04 (d, J=7.3 Hz, 1H), 6.83 (d, J=8.0 Hz, 1H), 6.49 (d, J=9.0 Hz, 1H), 6.43 - 6.27 (m, 2H), 5.36 - 5.27 (m, 1H), 4.11 (t, J=6.9 Hz, 2H), 3.51 - 3.30 (m, 2H), 2.93 - 2.64 (m, 5H), 2.60 (t, J=6.0 Hz, 2H), 1.79 - 1.69 (m, 2H), LC-MS (Acq~2min_TFA) tR = 0.71 mins, [M+H$^+$] = 487

3-(4-Phenoxyphenyl)-3-((5-(2-(5,6,7,8-tetrahydro-1,8-naphthyridin-2-yl)ethoxy)pyridin-2-yl)amino)propanoic acid (36), prepared by general procedure C using 4-phenoxybenzaldehyde. ^{1}H NMR (400 MHz, MeOD) δ ppm = 7.62 - 7.58 (m, 1H), 7.40 (d, J=8.8 Hz, 2H), 7.33 (s, 2H), 7.26 (d, J=7.3 Hz, 1H), 7.16 - 7.06 (m, 2H), 6.95 (d, J=7.8 Hz, 2H), 6.91 (d, J=8.5 Hz, 2H), 6.49 (dd, J=8.3, 16.6 Hz, 2H), 5.12 (t, J=6.8 Hz, 1H), 4.17 (t, J=6.5 Hz, 2H), 3.43 - 3.38 (m, 2H), 2.96 (t, J=6.4 Hz, 2H), 2.78 - 2.70 (m, 4H), 1.94 - 1.86 (m, 2H). Three exchangeable protons not observed, LC-MS (XBR~5min_HpH) tR = 2.42 mins, [M+H$^+$] = 511

General procedure D: Trifluoroborate salt coupling, hydrolysis

3-(3-(Morpholinomethyl)phenyl)-3-((5-(2-(5,6,7,8-tetrahydro-1,8-naphthyridin-2-yl)ethoxy)pyridin-2-yl)amino)propanoic acid (37) In a microwave vial was 1,1-dimethylethyl 7-(2-{[6-({1-(3-

bromophenyl)-3-[(1,1-dimethylethyl)oxy]-3-oxopropyl}amino)-3-pyridinyl]oxy}ethyl)-3,4-dihydro-1,8-naphthyridine-1(2H)-carboxylate (120 mg, 0.184 mmol), tri-tert-butylphosphane (0.092 ml, 0.092 mmol), XPhos (26.3 mg, 0.055 mmol), Cs_2CO_3 (179 mg, 0.551 mmol), $Pd(OAc)_2$ (4.12 mg, 0.018 mmol) and (morpholinium-4-ylmethyl)trifluoroborate internal salt (114 mg, 0.551 mmol) in THF (4 mL) and the reaction mixture was heated to 130 ^oC for 30 mins. The reaction mixture was then partitioned between DCM (50 mL) and H_2O (50 mL), the aq. phase was washed with further DCM (50 mL) and the combined organic phases were concentrated *in vacuo* and purififed by silica chromatography, eluting with EtOAc:cyclohexane (0 – 100 % EtOAc). The appropriate fractions were then concentrated *in vacuo* to give an oil. This was dissolved in DCM (3 mL) and 4M HCl in 1,4-dioxane (1 mL, 4.00 mmol) and two drops of H_2O were added and the reaction mixture stirred at rt for 18 h. The reaction mixture was then concentrated *in vacuo* and dissolved in DMSO:MeOH (1 mL) and purified by mass directed autoprep on Xbridge column using MeCN:H_2O with an ammonium carbonate modifier. The solvent was dried under a stream of N_2 in the Radleys blowdown apparatus to give the title compound (3.5 mg, 4%). ^1H NMR (400 MHz, MeOD) δ ppm = 7.60 - 7.56 (m, 1H), 7.40 - 7.26 (m, 4H), 7.19 (d, J=7.3 Hz, 1H), 7.09 (dd, J=3.0, 9.0 Hz, 1H), 6.53 (d, J=7.3 Hz, 1H), 6.42 (d, J=9.0 Hz, 1H), 5.13 (t, J=6.8 Hz, 1H), 4.14 (t, J=6.4 Hz, 2H), 3.64 (t, J=4.6 Hz, 4H), 3.60 (s, 2H), 3.44 - 3.38 (m, 2H), 2.99 (t, J=6.4 Hz, 2H), 2.79 - 2.71 (m, 4H), 2.53 - 2.45 (m, 4H), 1.90 (quin, J=5.9 Hz, 2H). Three exchangeable protons not observed, LC-MS (XBR~5min_HpH) tR = 2.00 mins, $[M+H^+]$ = 518

3-(4-(Morpholinomethyl)phenyl)-3-((5-(2-(5,6,7,8-tetrahydro-1,8-naphthyridin-2-yl)ethoxy)pyridin-2-yl)amino)propanoic acid (38), prepared by general procedure D using (morpholinium-4-ylmethyl)trifluoroborate internal salt. ^1H NMR (400 MHz, MeOD) δ ppm = 7.61 - 7.54 (m, 1H), 7.42 - 7.36 (m, 2H), 7.33 - 7.26 (m, 3H), 7.07 (dd, J=3.0, 9.0 Hz, 1H), 6.52 (d, J=7.3 Hz, 1H), 6.41 (d, J=9.0 Hz, 1H), 5.13 (t, J=6.9 Hz, 1H), 4.13 (t, J=6.4 Hz, 2H), 3.73 - 3.66 (m, 4H), 3.61 (s, 2H), 3.44 - 3.37 (m, 2H), 2.98 (t, J=6.4 Hz, 2H), 2.76 - 2.69 (m, 4H), 2.57 (d, J=4.0 Hz, 4H), 1.89 (quin, J=5.9 Hz, 2H). Three exchangeable protons not observed, LC-MS (XBR~5min_HpH) tR = 1.99 mins, $[M+H^+]$ = 518

3-(3-Cyclopropylphenyl)-3-((5-(2-(5,6,7,8-tetrahydro-1,8-naphthyridin-2-yl)ethoxy)pyridin-2-yl)amino)propanoic acid (39), prepared by general procedure C using 3-cyclopropylbenzaldehyde. ^{1}H NMR (400 MHz, DMSO-d6) δ = 12.19 (br. s, 1H), 7.65 (d, J = 3.4 Hz, 1H), 7.13 - 7.09 (m, 3H), 7.07 (dd, J = 3.2, 9.0 Hz, 1H), 7.03 (d, J = 7.3 Hz, 1H), 6.87 - 6.83 (m, 1H), 6.60 (br s, 1H), 6.44 (d, J = 8.8 Hz, 1H), 6.33 (d, J = 7.3 Hz, 1H), 6.29 (br s, 1H), 5.18 (br s, 1H), 4.11 (t, J = 6.8 Hz, 2H), 3.26 - 3.19 (m, 2H), 2.80 (t, J = 6.8 Hz, 2H), 2.73 (dd, J = 8.3, 15.7 Hz, 1H), 2.63 - 2.54 (m, 3H), 1.85 (tt, J = 5.1, 8.4 Hz, 1H), 1.74 (quin, J = 5.9 Hz, 2H), 0.95 - 0.87 (m, 2H), 0.65 - 0.57 (m, 2H), ^{13}C NMR (101 MHz, DMSO-d6) δ = 172.18, 155.83, 153.73, 153.06, 146.91, 143.75, 143.36, 135.93, 133.66, 127.94, 125.86, 123.81, 123.55, 123.34, 112.82, 110.63, 108.75, 68.32, 51.88, 42.17, 40.62, 37.02, 25.98, 20.93, 15.05, 9.32, 9.30, LC-MS (XBR~5min_HpH) tR = 2.24 mins, [M+H+] = 459, HR-MS: calc for C27H31N4O3 (M+H)+ 459.2396, found 459.2400.

General procedure E: Suzuki cross coupling

3-(3,5-Dicyclopropylphenyl)-3-((5-(2-(5,6,7,8-tetrahydro-1,8-naphthyridin-2-yl)ethoxy)pyridin-2-yl)amino)propanoic acid (40), A mixture of cyclopropylboronic acid (70.4 mg, 0.819 mmol), tert-butyl 7-(2-((6-((3-(tert-butoxy)-1-(3,5-dibromophenyl)-3-oxopropyl)amino)pyridin-3-yl)oxy)ethyl)-3,4-dihydro-1,8-naphthyridine-1(2H)-carboxylate (100 mg, 0.137 mmol), tripotassium phosphate (174 mg, 0.819 mmol), 2'-(dimethylamino)-2-biphenylyl-palladium(II) chloride dinorbornylphosphine complex (15.30 mg, 0.027 mmol) in 1,4-Dioxane (5 mL) and H_2O (0.5 mL) was heated in a sealed tube in a Biotage Initiator microwave using initial normal absorption level setting to 130 °C for 30 min. 4M HCl in 1,4-dioxane (0.068 mL, 0.273 mmol) was added and the reaction mixture was stirred for 4 h. H_2O (5 mL) and DCM (5 mL) were then added and the organic layer was extracted. 4M HCl in 1,4-dioxane (0.5 mL) was added to the organic layer. The reaction mixture was then stirred for 2 h at rt before being concentrated *in vacuo* to give a brown gum. This was dissolved in DMSO (1 mL) and purified by Mass Directed AutoPrep on Xbridge column using MeCN: H_2O with an ammonium carbonate modifier. The solvent was dried under a stream of N_2 in the Radleys blowdown apparatus to give the target

compound (4.3 mg, 6%). ^{1}H NMR (400 MHz, MeOD) δ ppm = 7.62 (br. s., 1H), 7.33 (d, J=7.1 Hz, 1H), 7.14 (d, J=8.3 Hz, 1H), 6.93 - 6.86 (m, 2H), 6.69 - 6.60 (m, 1H), 6.55 (d, J=7.1 Hz, 1H), 6.49 - 6.38 (m, 1H), 5.10 - 4.97 (m, 1H), 4.24 - 4.11 (m, 2H), 3.49 - 3.38 (m, 3H), 3.08 - 2.93 (m, 2H), 2.81 - 2.71 (m, 3H), 1.98 - 1.75 (m, 4H), 0.90 (s, 4H), 0.62 (s, 4H). Three exchangeFable protons not observed, LC-MS (Acq~2min_HpH) tR = 0.93 mins, [M+H^{+}] = 499

Small Molecule X-ray Crystallography

Single enantiomer **32** was crystallized by slowly evaporating a DMSO solution to give a 1:1 solvate. All measurements were made at 150(2) K using an Oxford Diffraction Gemini A Ultra diffractometer equipped with an Enhance (Mo) X-ray source (λ = 0.71073 Å). A Gaussian absorption correction was applied based on measured crystal faces. The structure was solved and refined by full-matrix least squares procedures using the SHELXTL V2008/4 package (Bruker, 2008). Co-ordinates and anisotropic atomic displacement parameters were refined for all non-hydrogen atoms. For the hydrogens associated with the nitrogen atoms, atomic co-ordinates and isotropic atomic displacement parameters were freely refined. All other hydrogen atoms were included in calculated positions and were refined using the riding mode. Isotropic atomic displacement parameters for these hydrogens were used as appropriate multiples of Ueq for the attached carbon atom. Further details of this data collection and refinement can be found in the crystallographic information file (CIF) deposited as ESI, together with the checkCIF output. The CIF and FCF files were also deposited with the Cambridge Crystallographic Data Centre (CCDC 1919504).

ASSOCIATED CONTENT

Supporting Information

The Supporting Information is available free of charge on the ACS Publications website at DOI: XXX.

General experimental information; full synthetic procedures and characterisation data for all new compounds; NMR and LC-MS data, molecular formula strings and biological data, experimental

procedure for artificial membrane permeability assay, fluorescence polarization assays, computational details and small molecule X-ray crystallography. Two .mol2 files containing docked poses for compounds **3** and **39** in αvβ6 and αvβ3 respectively.

All animal studies were ethically reviewed and carried out in accordance with Animals (Scientific Procedures) Act 1986 and the GSK Policy on the Care, Welfare and Treatment of Animals.

AUTHOR INFORMATION

Corresponding Author

*E-mail: niall.a.anderson@GSK.com.

ORCID

Niall Anderson: 0000-0001-8403-9698

Present Addresses

≠S.C. Pharmaron, Drug Discovery Services Europe, Hertford Road, Hoddesdon, Hertfordshire EN11 9BU, U.K.

Author contributions: The manuscript was written by NAA, SAC and SJFM. All authors have given approval to the final version of the manuscript.

Conflict of Interest: The authors are shareholders in GlaxoSmithKline.

Acknowledgments

We thank Seb Campos who wrote the first draft of this manuscript, James Thompson for compound resynthesis and Professor W. Clegg and Dr. R. W. Harrington from the University of Newcastle for the GSK funded crystal structure of **32**.

Abbreviations used

IPF, idiopathic pulmonary fibrosis; RGD, arginine-glycine-aspartic acid; FP, fluorescence polarisation; SAR, structure activity relationship; MIDAS, metal ion dependent adhesion site.

Accession Codes

PDB codes for docking of compounds **3** and **39** into crystal structures: Figure 2 and Figure 4: αvβ6 - 4UM9, Figure 5: αvβ3 – 1L5G. Authors will release the atomic coordinates and experimental data upon article publication. CCDC deposit number for small molecule crystal structure of compound **32** is 1919504.

REFERENCES

[1] Friedman, S.L.; Sheppard, D.; Duffield, J.S.; Violette, S. Therapy for Fibrotic Diseases: Nearing the Starting Line. *Science Trans. Med*. **2013**, *5*, 1-17.

[2] Selman, M.; Pardo, A.; Richeldi, L.; Cerri, S. Emerging Drugs for Idiopathic Pulmonary Fibrosis. *Expert Opin. Emerging Drugs* **2011**, *16*, 341-362.

[3] El-Chemaly, S.; Pacheco-Rodriguez, G.; Ikeda, Y.; Malide, D.; Moss, J. Lymphatics in Idiopathic Pulmonary Fibrosis: New Insights into an Old Disease. *Lymphatic Res. Biol*. **2009**, *7*, 197-203.

[4] Hubbard, R.; Venn, A.; Smith, C.; Cooper, M.; Johnston, I.; Britton, A. J. Exposure to Commonly Prescribed Drugs and the Etiology of Cryptogenic Fibrosing Alveolitis. *Am. J. Respir. Crit. Care Med*. **1998**, *157*, 743-747.

[5] Gribbin, J.; Hubbard R.B.; Le Jeune I.; Smith, C.J.P.; West, J.; Tata, L.J. Incidence and Mortality of Idiopathic Pulmonary Fibrosis and Sarcoidosis in the UK. *Thorax* **2006**, *61*, 980-985.

[6] Vancheri, C.; Failla, M.; Crimi, N.; Raghu, G. Idiopathic Pulmonary Fibrosis: a Disease with Similarities and Links to Cancer Biology. *Eur. Respir. J*. **2010**, *35*, 496-504.

[7] Du Bois, R.M. Strategies for Treating Idiopathic Pulmonary Fibrosis. *Nat. Rev. Drug Discovery* **2010**, *9*, 129-140.

[8] Navaratnam, V.F.; West, J.; Smith, C.J.P.; Jenkins, R.G; Fogarty, A; Hubbard, R. The Rising Incidence of Idiopathic Pulmonary Fibrosis in the U.K. *Thorax* **2011**, *66*, 462-467.

[9] Jenkins, G. Pirfenidone Should Be Prescribed for Patients with Idiopathic Pulmonary Fibrosis. *Thorax* **2013**, *68*, 603-605.

[10] Richeldi, L.; du Bois, R.M.; Raghu, G.; Azuma, A.; Brown, K.K.; Costabel, U.; Cottin, V.; Flaherty, K.R.; Hansell, D.M.; Inoue, Y.; Kim, D.S.; Kolb, M.; Nicholson, A.G.; Noble, P.W.; Selman, M.; Taniguchi, H.; Brun, M.; Le Maulf, F.; Girard, M.; Stowasser, S.; Schlenker-Herceg, R.; Disse, B.; Collard, H.R. Efficacy and Safety of Nintedanib in Idiopathic Pulmonary Fibrosis. *N. Engl. J. Med*. **2014**, *370*, 2071-2082.

[11a] Blobe, G.C.; Schiemann, W.P.; Lodish, H.F. Role of Transforming Growth Factor Beta in Human Disease. *N. Engl. J. Med*. **2000**, *342*, 1350-1358. [11b] Hynes, R.O. Integrins: Bidirectional, Review Allosteric Signaling Machines. *Cell* **2002**, *110*, 673-687. [11c] Humphries, M.J. Integrin Structure. *Biochem. Soc. Trans*. **2000**, *28*(*4*), 311-340.

[12a] Hatley, R.J.D.; Macdonald, S.J.F.; Slack, R.J.; Le, J.; Ludbrook, S.B.; Lukey, P.T. An αv-RGD Integrin Inhibitor Toolbox: Drug Discovery Insight, Challenges and Opportunities. *Angew. Chem., Int. Ed*. **2018**, *57*, 3298-3321. [12b] Sheldrake, H.M.; Patterson, L.H. Strategies to Inhibit Tumor Associated Integrin Receptors: Rationale for Dual and Multi-Antagonists. *J. Med. Chem*. **2014**, *57*, 6301−6315.

[13] Horan, G.S.; Wood, S.; Ona, V.; Li, D.J.; Lukashev, M.E.; Weinreb, P.H.; Simon, K.J.; Hahm, K.; Allaire, N.E.; Rinaldi, N.J.; Goyal, J.; Feghali-Bostwick, C.A.; Matteson, E.L.; O'Hara, C.; Lafyatis, R.; Davis, G.S.; Huang, X.; Sheppard, D.; Violette, S.M. Partial Inhibition of Integrin Alpha(v)Beta6 Prevents Pulmonary Fibrosis Without Exacerbating Inflammation. *Am. J. Respir. Crit. Care Med*. **2008**, *177*, 56-65.

[14] Munger, J.S.; Huang, X.; Kawakatsu, H.; Griffiths, M.J.; Dalton, S.L.; Wu, J.; Pitter, J.F.; Kaminski, N.; Garat, C.; Matthay, M.A.; Rifkin, D.B.; Sheppard, D. The Integrin Alpha v Beta 6 Binds and Activates Latent TGF Beta 1: A Mechanism for Regulating Pulmonary Inflammation and Fibrosis. *Cell* **1999**, *96*, 319-328.

[15] Wilkinson, A.L.; Barrett, J.W.; Slack, R.J. Pharmacological Characterisation of a Tool αvβ1 Integrin Small Molecule RGD-Mimetic Inhibitor. *Eur. J. Pharm.* **2019**, *842*, 239–247

[16] Conroy, K.P.; Kitto, L.J., Henderson, N.C. αv Integrins: Key Regulators of Tissue Fibrosis. *Cell Tiss. Res*. **2016**, *365*, 511-519 and Atabai, A.; Jame, S.; Azhar, N.; Kuo, A.; Lam, M.; McKleroy, W.; DeHart, G.; Rahman, S.; Xia, D.D.; Melton, A.C.; Wolters, P.; Emson, C.L.; Turner, S.M.; Werb, Z.; Sheppard, D. Mfge8 Diminishes the Severity of Tissue Fibrosis in Mice by Binding and Targeting Collagen for Uptake by Macrophages. *J. Clin. Invest.* **2009**, *119*, 3713-3722

[17] Teoh, C.M.; Tan, S.S.L.; Tran, T. Integrins as Therapeutic Targets for Respiratory Diseases. *Curr. Mol. Med.* **2015**, *15*, 714-734

[18] Henderson, N.; Arnold, T.D.; Katamura, Y.; Giacomini, M.M.; Rodriguez, J.D.; McCarty, J.H.; Pellicoro, A.; Raschperger, E.; Betsholtz, C.; Ruminski, P.G.; Griggs, D.W.; Prinsen, M.J.; Maher, J.J.; Iredale, J.P.; Lacy-Hulbert, A.; Adams, R.H.; Sheppard, D. Targeting of αv Integrin Identifies a Core Molecular Pathway that Regulates Fibrosis in Several Organs. *Nature Med*. **2013**, *19*, 1617-1624.

[19] Goodman, S.L.; Picard, M. Integrins as Therapeutic Targets. *Trends Pharmacol. Sci*. **2012**, *33*, 405-412.

[20] Kapp, T.G.; Rechenmacher, F.; Neubauer, S.; Maltsev, O.G.; Cavalcanti-Adam, E.A.; Zarka, R.; Reuing, U.; Notni, J.; Wester, H-G.; Mas-Moruno, C.; Spatz, B.; Geiger, B.; Kessler, H. A Comprehensive Evaluation of the Activity and Selectivity Profile of Ligands for RGD-Binding Integrins. *Sci. Reports*, **2017**, *7:39805*, 1-13.

[21] Miller, L.M.; Pritchard, J.M.; Macdonald, S.J.F.; Jamieson, C.; Watson, A.J.B. Emergence of Small Molecule Non-RGD-Mimetic Inhibitors for RGD Integrins. *J. Med. Chem*. **2017**, *60*, 3241-3251.

[22] Procopiou, P.A.; Anderson, N.A.; Barrett, J.; Barrett, T.N.; Crawford, M.H.J.; Fallon, B.J.; Hancock, A.P.; Le, J.; Lemma, S.; Marshall, R.P.; Morrell, J.; Pritchard, J.; Rowedder, J.E.; Saklatvala, P.; Slack, R.J.; Sollis, S.L.; Suckling, C.J.; Thorp, L.R.; Vitulli, G.; Macdonald, S.J.F. Discovery of (S)-3-(3-(3,5-Dimethyl-1H-pyrazol-1-yl)phenyl)-4-((R)-3-(2-(5,6,7,8-tetrahydro-1,8-naphthyridin-2-yl)ethyl)pyrrolidin-1-

yl)butanoic Acid, a Nonpeptidic αvβ6 Integrin Inhibitor for the Inhaled Treatment of Idiopathic Pulmonary Fibrosis. *J. Med. Chem*. **2018**, *61*, 8417-8443.

[23] Miller, W.H.; Manley, P.J.; Cousins, R.D.; Erhard, K.F.; Heerding, D.A.; Kwon, C.; Ross, S.T.; Samanen, J.M.; Takata, D.T.; Uzinskas, I.N.; Yuan, Catherine C.K.; Haltiwanger, R.; Curtis; G., Catherine J.; Lark, M.W.; Hwang, S.M.; James, I.E.; Rieman, D.J.; Willette, R.N.; Yue, T.L; Azzarano, L.M.; Salyers, K.L.; Smith, B.R.; Ward, K.W.; Johanson, K.O.; Huffman, W.F. Phenylbutyrates as Potent, Orally Bioavailable Vitronectin Receptor (Integrin αvβ3) Antagonists. *Bio. Med. Chem. Let*. **2003**, *13*, 1483-1486.

[24] Adams, J.; Anderson, E.C.; Blackham, E.E.; Chiu, Y.W. R.; Clarke, T.; Eccles, N.; Gill, L.A.; Haye, J.J.; Haywood, H.T.; Hoenig, C.R.; Kausas, M.; Le, J.; Russell, H.L.; Smedley, C.; Tipping, W.J.; Tongue, T.; Wood, C.C.; Yeung, J.; Rowedder, J.E.; Fray, M.J.; McInally, T.; Macdonald, S.J.F. Structure Activity Relationships of αv Integrin Antagonists for Pulmonary Fibrosis by Variation in Aryl Substituents. *ACS Med. Chem. Lett*. **2014**, *5*, 1207-1212.

[25] Friesner, R.A.; Murphy, R.B.; Repasky, M.P.; Frye, L.L.; Greenwood, J.R.; Halgren, T.A.; Sanschagrin, P.C.; Mainz, D.T., Extra Precision Glide: Docking and Scoring Incorporating a Model of Hydrophobic Enclosure for Protein-Ligand Complexes. *J. Med. Chem*. **2006**, *49*, 6177–6196.

[26] Halgren, T.A.; Murphy, R.B.; Friesner, R.A.; Beard, H.S.; Frye, L.L.; Pollard, W.T.; Banks, J.L. Glide: A New Approach for Rapid, Accurate Docking and Scoring. 2. Enrichment Factors in Database Screening. *J. Med. Chem*. **2004**, *47*, 1750–1759.

[27] Friesner, R.A.; Banks, J.L.; Murphy, R.B.; Halgren, T.A.; Klicic, J.J.; Mainz, D.T.; Repasky, M.P.; Knoll, E.H.; Shaw, D.E.; Shelley, M.; Perry, J.K.; Francis, P.; Shenkin, P.S., Glide: A New Approach for Rapid, Accurate Docking and Scoring. 1. Method and Assessment of Docking Accuracy. *J. Med. Chem*. **2004**, *47*, 1739–1749.

[28] Dong, X.; Hudson, N.E.; Lu, C.; Springer, T.A. Structural Determinants of Integrin β-Subunit Specificity for Latent TGF. *Nature Struct. Mol. Biol*. **2014**, *21*, 1091-1097.

[29] Fyfe, J.W.B.; Watson, A.J.B. Recent Developments in Organoboron Chemistry: Old Dogs, New Tricks. *Chem.* **2017**, *3*, 31–55.

[30] Coleman, P.J.; Brashear, K.M.; Askew, B.C.; Hutchinson, J.H.; McVean, C.A.; Duong, L.T.; Feuston, B.P.; Fernandez-Metzler, C.; Gentile, M.A.; Hartman, G.D.; Kimmel, D.B.; Leu, C.-T.; Lipfert, L.; Merkle, K.; Penny-packer, B.; Prueksaritanont, T.; Rodan, G.A.; Wesolowski, G.A.; Rodan, S.B.; Duggan, M.E. Nonpeptide αvβ3 Antagonists. Part 1: Discovery and Preclinical Evaluation of Potent αvβ3 Antagonists for the Prevention and Treatment of Osteoporosis. *J. Med. Chem*. **2004**, *47*, 4829-4837.

[31] Xiong J.P; Stehle T.; Zhang R.; Joachimiak A.; Frech M.; Goodman S.L.; Arnaout M.A. Crystal Structure of the Extracellular Segment of Integrin Alpha v Beta 3 in Complex with an Arg-Gly-Asp Ligand. *Science* **2002**, *296*, 151-155.

[32] IV arm: DMSO : PEG200 : water 5:45:50 v/v/v, dosed at 1 mL/kg. Oral arm: 0.5% aq methyl cellulose (w/v) containing 0.2% Tween 80, dosed at 10 mL/kg.

TABLE OF CONTENTS GRAPHICS

Optimisation of a series of pan αv integrin antagonists

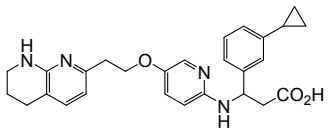

Excellent binding affinity in fluorescence polarisation assays

αvβ3 = 4 nM
αvβ5 = 4 nM
αvβ6 = 16 nM
αvβ8 = 40 nM

Good rat pharmacokinetic profile for oral delivery

Cl = 8 mL/min/kg
Vss = 0.5 L/kg
T1/2 = 1.8 h
Oral F = 98%

Docking into a crystal structure of αvβ6